Responses to referee comments on**, "Modeling Total Electron Content derived from radio occultation measurements by COSMIC satellites over the African Region"**

By Mungufeni et al.

May 03, 2020

We thank the editor and reviewers for taking time to evaluate our manuscript. All the comments are addressed as shown below.

Editor:

Thank you for submitting your manuscript to Annales Geophysicae and for your response to the referees' comments. The study you are reporting is interesting contribution to the knowledge of the coupling of the solar wind-magnetosphere-ionosphere system over the African region. However, as you already know, the referees had some important objections to the present version of the manuscript, and this is a reason why I am suggesting a major revision. From my side, I suggest to make reference in the improved manuscript the already published paper by Okoh et al (2019) and introduce brief comparison of the approaches and finding presented in both your and Okoh's paper. Please, consider carefully and discuss in the revised version of the manuscript all comments of the referees indicating the changes you have newly introduced. The manuscript will be revised once again. If you are prepared to undertake the improvements required, please submit the revised manuscript.

Response:

The paper by Okoh et al., (2019) has been cited and discussed in the revised version of the manuscript on page 4, lines 15 – 23; page 5, lines 12 – 22; page 8, lines 2 – 7; pages 22 – 24, page 29, lines 14 - 18. Comparison of approaches and findings presented in our paper and that of Okoh et al., (2019) can be deduced from text on page 4, lines 15 – 26; page 5, lines 12 – 22; and pages 22 - 24. The highlights of the comparisons and findings are as follows.

Differences between approaches in Okoh et al., (2019) and the current study		
	Okoh et al., (2019)	Current study
1	used neural network technique to develop TEC model over the entire African region.	used B spline functions to model TEC over the entire African region.
2	Used both adjusted COSMIC RO TEC and ground-based GPS TEC	Used only COSMIC RO TEC without adjustment

Findings:

Due to the lack of a dense network of ground-based GNSS receivers and poor coverage of COSMIC RO data over the African region, the TEC model over the entire African region presented by Okoh et al. (2019) sometimes failed to capture the equatorial ionization anomaly (EIA) over the region. This point has been illustrated with examples in this document on page 7. To overcome poor coverage of COSMIC RO data, the current study applied data binning method that allowed development of an improved TEC model over the region. Another reason we suspect that might have resulted in TEC maps based on Okoh et al., (2019) not yielding the EIA feature sometimes could be discrepancy between two data sets which were used. i.e adjusted COSMIC RO TEC and ground-based GPS TEC. We illustrate in this document on pages 5 and 6 the possible reason for the shortfall in the adjustment of COSMIC RO TEC. Based on these issues, this study only used COSMIC RO TEC without adjustment. Since this data comprised of electron density up to ~800 km, our model was able to reproduce equivalent TEC observed by ionosonde stations. On the other hand, the model of Okoh et al., (2019) can yield equivalent TEC observed by ground-based GPS receivers.

Comments by the reviewers are addressed as shown below.

Responses to Reviewer #1

Comment:

An author of this paper (Patrick Mungufeni) along with a long list of other authors have recently published the following paper: Okoh, et al. (2019). A neural network based ionospheric model over Africa from COSMIC and Ground GPS observations. Journal of Geophysical Research: Space Physics, 124. https://doi.org/10.1029/2019JA027065. In that particular paper the authors perform an adjustment using Neural Networks according to which they correct the reasonable discrepancy between TEC from ground based receivers (up to 22000 Km) and occultation measurements up to 700 Km. They seem to apply no such procedure in this paper. This is a major problem of this paper. They also need to make special reference to that paper.

Response:

The preceding response (to the editor) specifies page and line numbers where citations and discussions of Okoh et al. (2019) within the current version of the manuscript can be seen. The numerous cases of citations and discussions signify a special mention of Okoh et al. (2019). While we agree to the reviewer's recommendation to create a data base consisting of both ground and space based TEC measurements, such data base may be subjected to several other issues and criticisms. These issues have been discussed in the revised manuscript in page 5, lines 12 – 22; page 8, lines 5 – 7.

More explanations which could not be put in the manuscript due to space constraints are provided below.

Indeed, Patrick Mungufeni contributed to the paper in the comment which was published on Thur, Dec 12, 5:23 PM. The current manuscript was first submitted on Saturday, Nov 23, 2:09 PM (Korean time). Therefore, we could not reference Okoh et al,

(2019) since it was published later after our first submission. Below are the screen shots of emails to prove the dates.

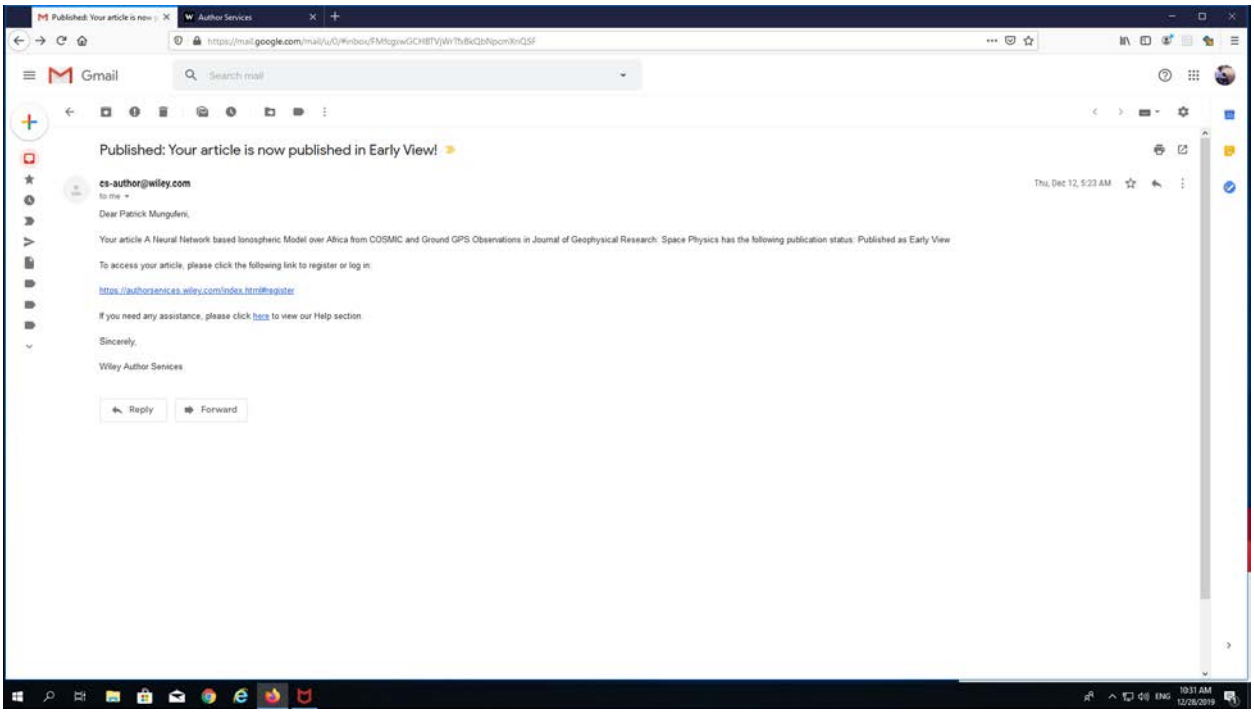

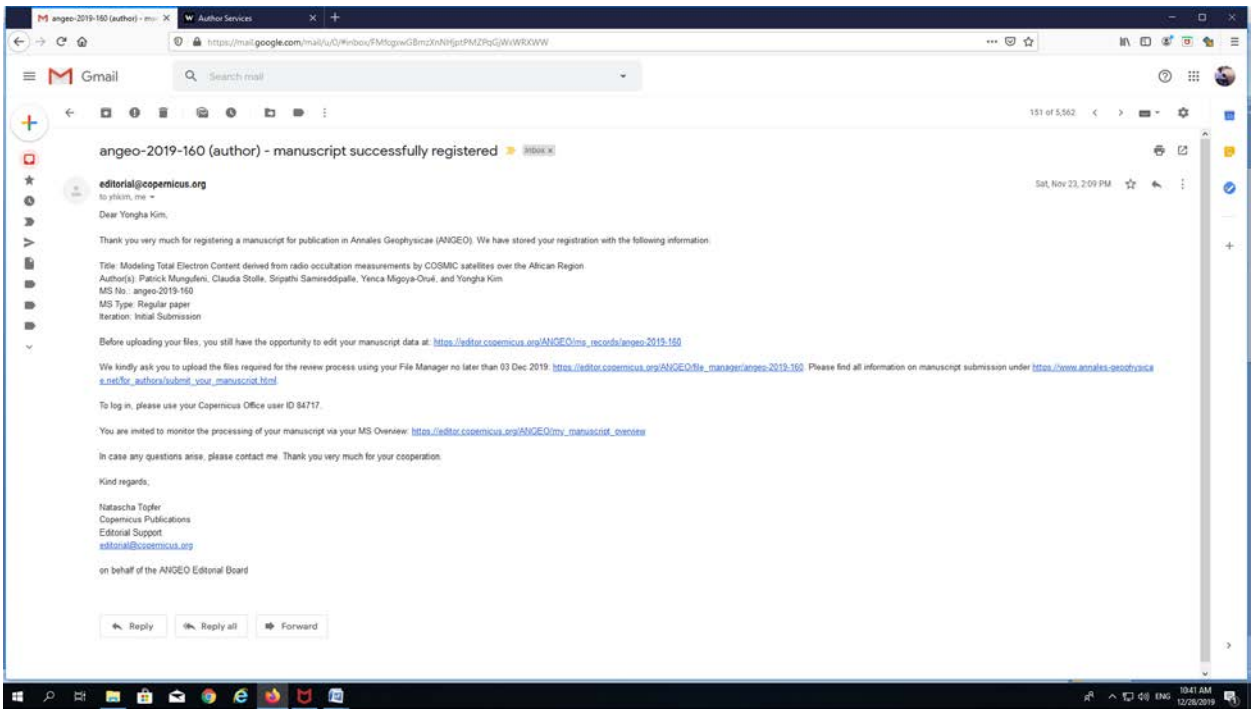

Although the reviewer is recommending creation of data base consisting of both ground and space based TEC measurements, such data base may be subjected to criticism. For example, the observation in Okoh et al. (2019) where the ratio between ground based and COSMIC TEC varies spatially implies that neural network may not learn the relationship between the two data sets over locations which only have COSMIC TEC data. We have highlighted with magenta boxes in Figure below such regions which mostly have COSMIC TEC. The Figure was taken from Okoh et al. (2019). Over the boxes, the adjustments made to COSMIC TEC may not be trusted because of large distances over which interpolations are done.

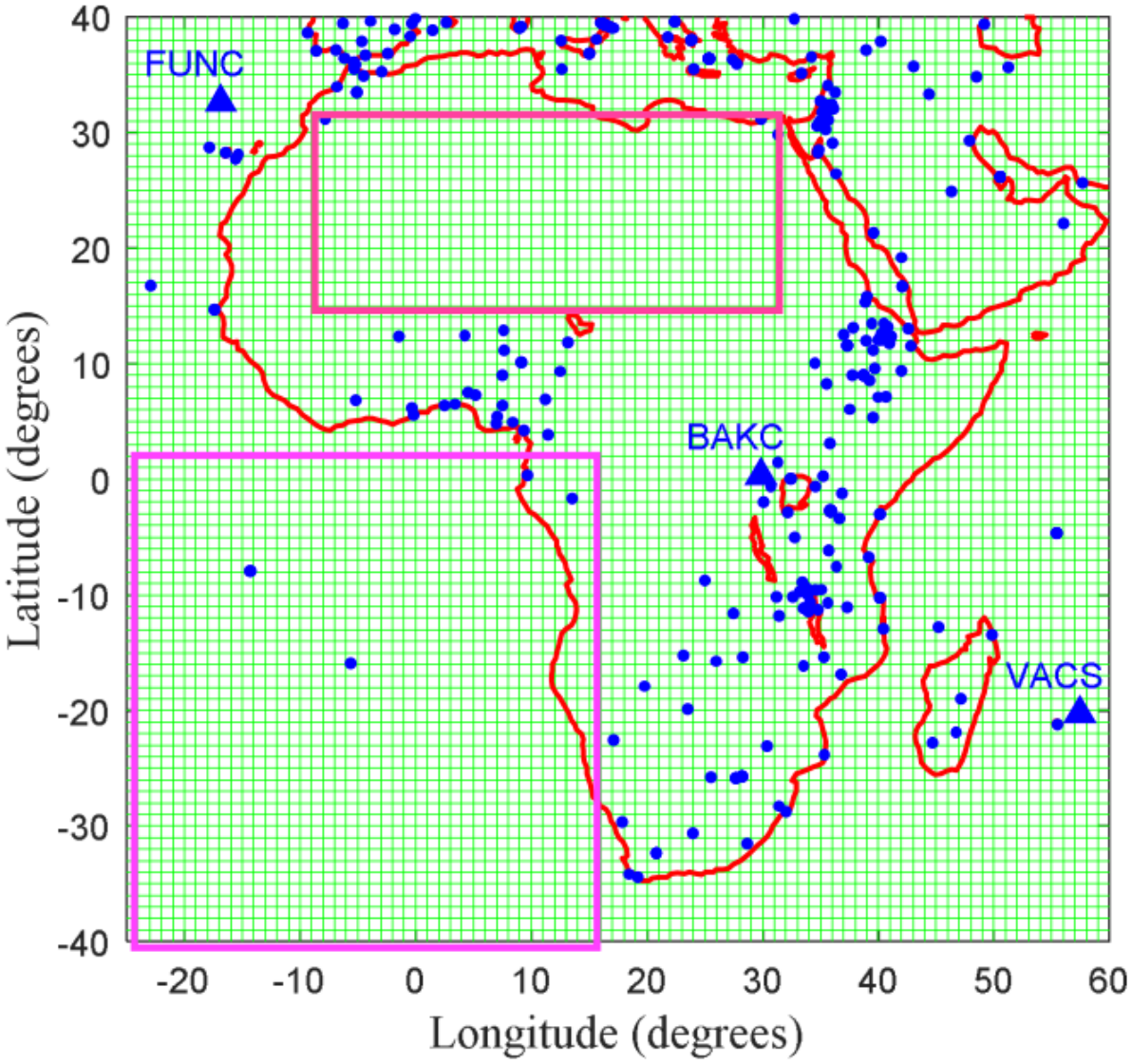

When a study opts to have both adjusted COSMIC TEC data and ground based GPS TEC data, some locations will be represented by adjusted COSMIC TEC (remember not trusted) while others will be represented by ground based GPS TEC. Obviously, there is still disparity. For purposes of consistency, it might be fair to use entirely adjusted COSMIC TEC since it can also be available where there is ground based GPS TEC. Unlike in Okoh et al. (2019) and Mungufeni et al. (2019), the current manuscript used only COSMIC TEC without any adjustment.

Comment:

May be they should compare the output of the NN model out of that paper with the output of the spline model for this paper despite that the COSMIC dataset is used as a basis for both models. In this way they will prove their approach for this paper (omitting any correction for the plasmaspheric contribution which is expected to be high at middle African latitudes.

Response:

In pages 22 - 24, we have presented comparison between NN TEC maps and spline technique TEC maps. As indicated in Okoh et al. 2019, TEC plots based on NN model can be obtained from MATLAB Central website (https://www.mathworks.com/matlabcentral/fileexchange/69257-african-gnss-tec-afritec-model?s_tid=prof_contriblnk). We present in Figure below examples of TEC generated by NN model at 11 UT on DOY 81 (March), 171 (June), 260 (September), and 347 (December) of the year 2012.

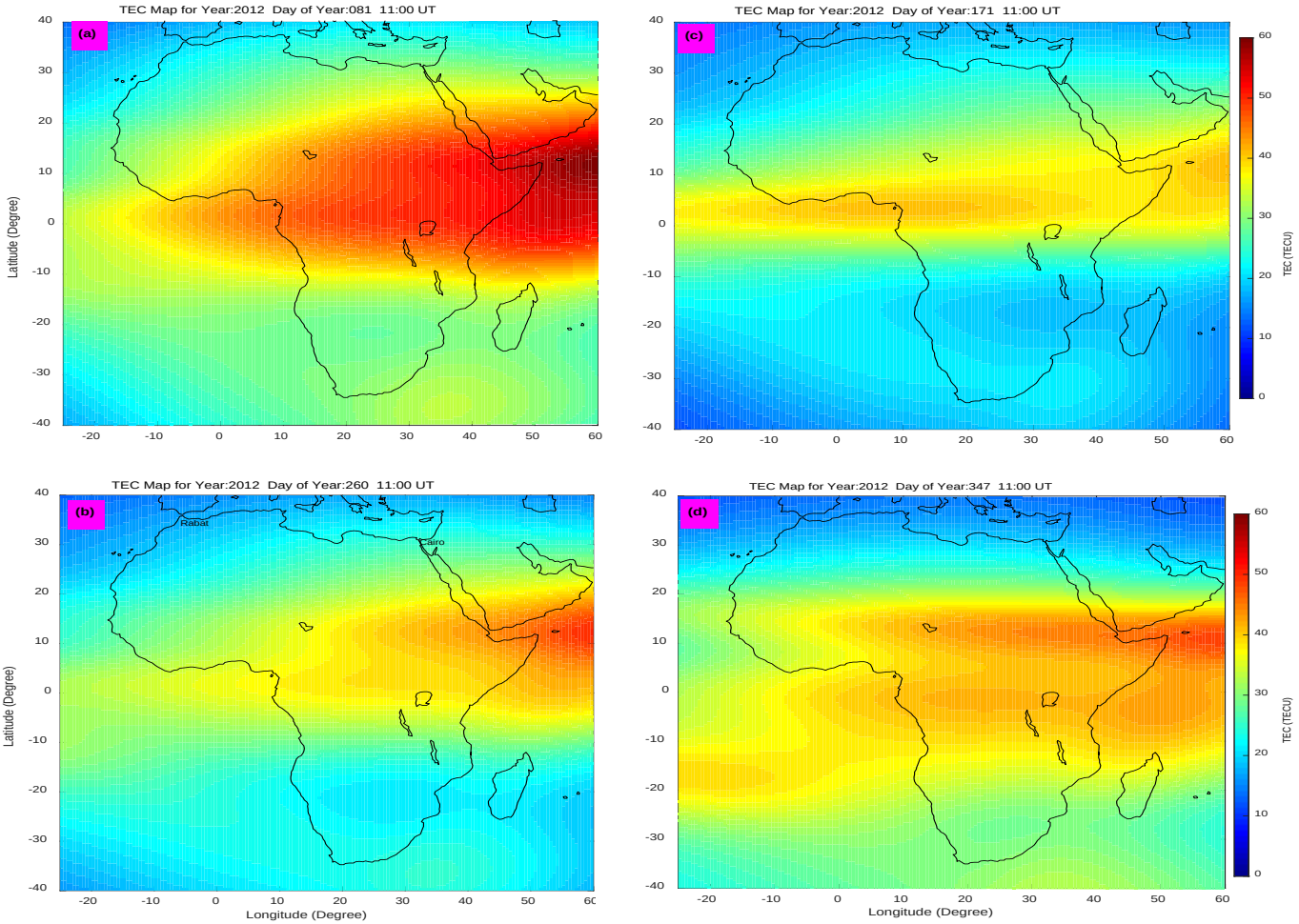

The corresponding TEC maps generated based on our model (spline method) are presented below.

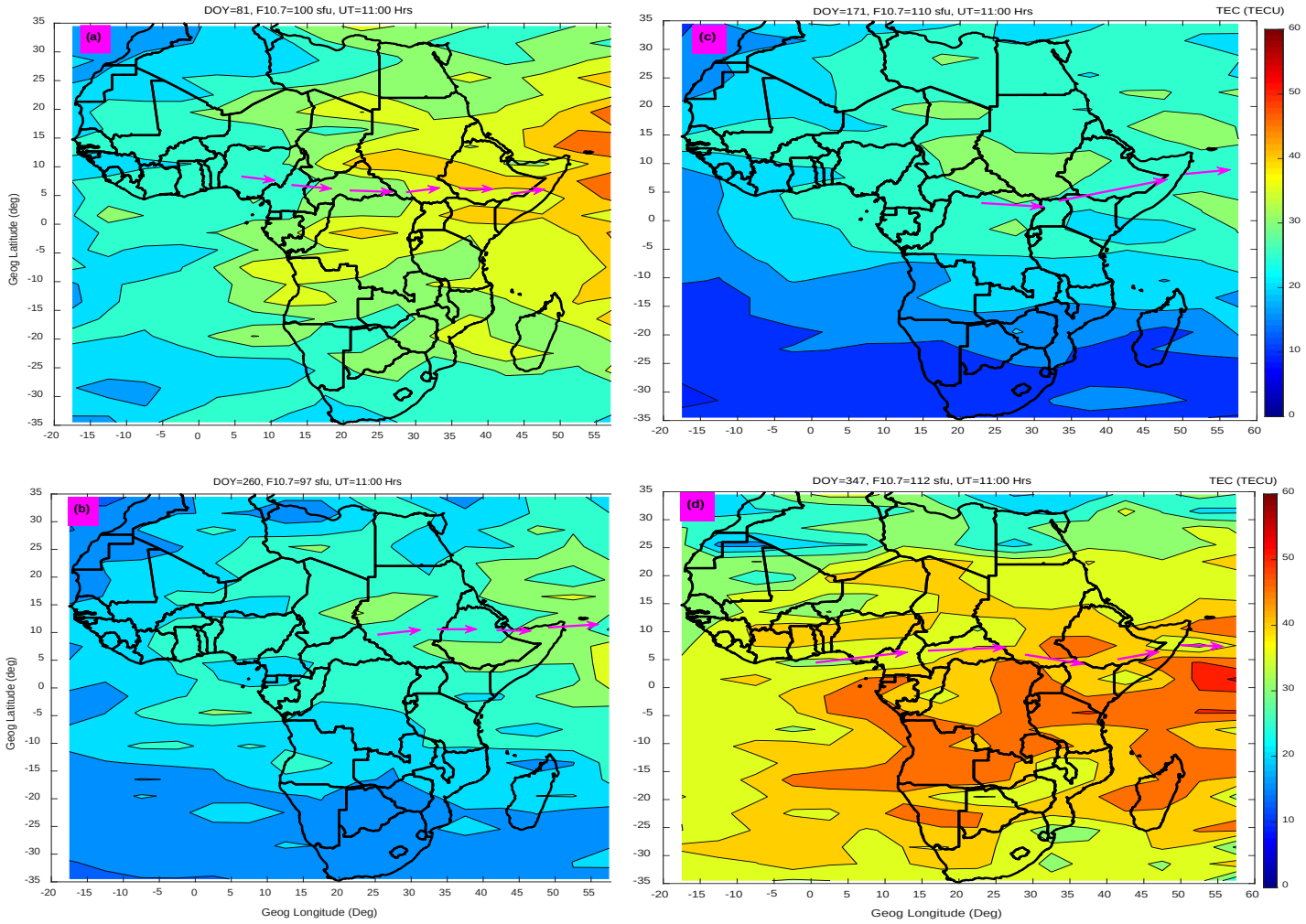

Unlike our TEC maps which clearly show the EIA trough (see magenta arrows) in all the seasons, the neural network technique TEC maps only clearly capture the EIA trough in December solstice. As pointed before, this short fall in neural network TEC model might be due to poor amount of data to represent day of year during model development and discrepancy between the two data sets (adjusted COSMIC RO TEC and ground-based GPS TEC) used in the study. Another observation that can be made from above two sets of figures is that unlike the neural network model which yields smooth spatial TEC variation, the spline modeling technique does not yield smooth spatial TEC variation. In real life, measurement or observed values rarely vary smoothly. Since the spline modeling technique produces results (see Figure 1 of revised manuscript) which

demonstrate that the modeled data matches almost perfectly the observed data, it is expected that the spatial variations of TEC in maps of spline model are not smooth.

It would be interesting to compare error levels produced when some measured TEC is compared with (i) NN TEC map and (ii) our spline model. We may not perform such analysis since model in (i) is based on electron density that is integrated from ground up to GPS satellites, while model in (ii) is based on electron density integrated up to ~800 km.

Comment:

The authors do not provide any scheme by which they would reject any unrealistic COSMIC profiles. There have been numerous validation studies with Digisondes that verify this problem especially in the bottomside.

Response:

Justifications for not rejecting some of the values are discussed in page 7, lines 14 – 18, page 8, lines 1 - 22. Due to space limits in the manuscript, we could not include the following analysis.

Empirical modeling requires adequate data for the mathematical functions to capture the physics inherent in the data. However, to minimize measurement errors, studies that have used COSMIC data commonly reject measurements with horizontal smear > 1500 km. We have presented in Figure below the number of COSMIC TEC measurements per day during the year 2013 over the longitude and latitude ranges of -15 – 60^{o} and -35 – 35^{o}, respectively.

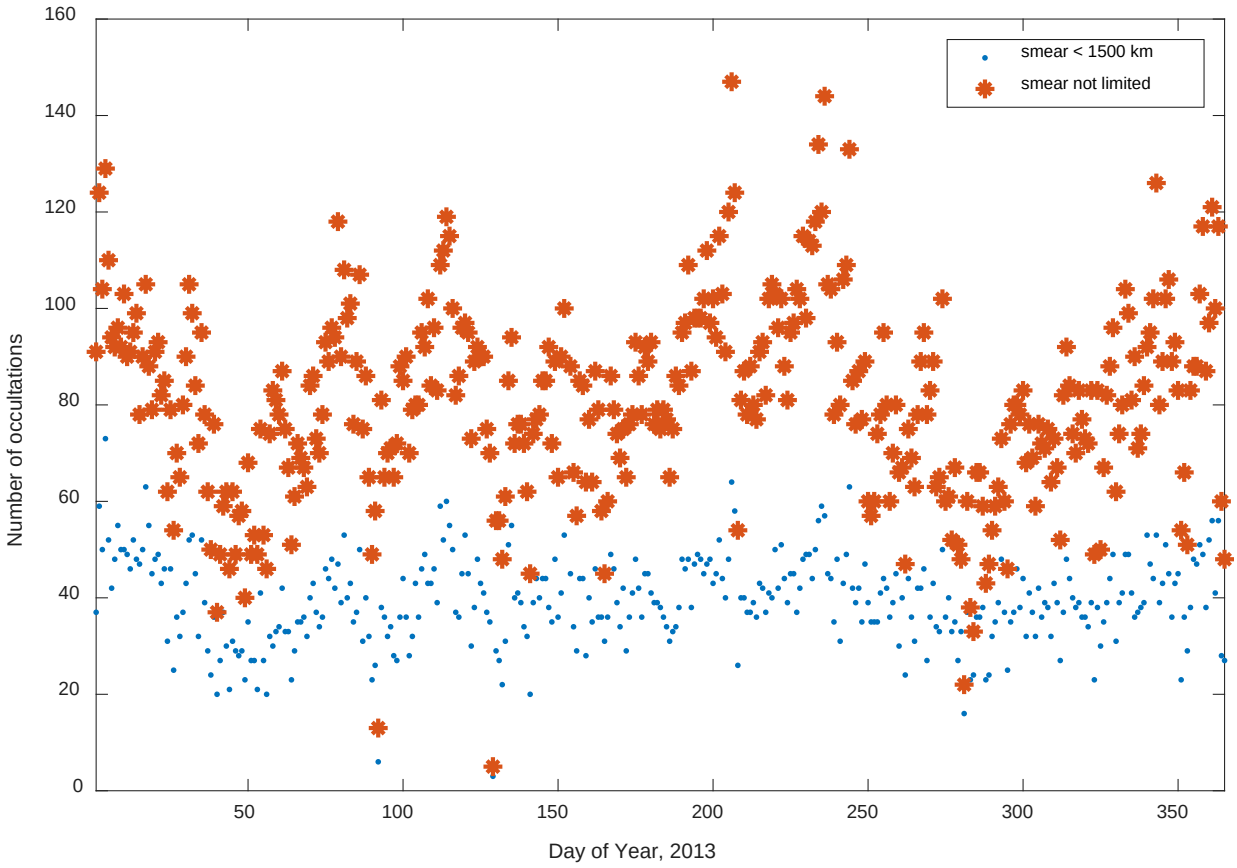

The blue dots indicate COSMIC TEC measurements when the horizontal smear is < 1500 km, while the red stars indicate COSMIC TEC measurements without limitation of horizontal smear. It can be noticed that when the horizontal smear is limited, ~40 observations may be made per day. Obviously, the 40 measurements may not cover very well all the 24 hours in a day and all the grid cells. In the revised manuscript, there are 9,216 (16 longitudinal, 24 latitudinal, and 24 local time) grid cells arising from 5^{o} lon, 3^{o} lat, and 1 hr LT binning resolutions. Comparison of the numbers 40 and 9,216 shows clearly that the seasonal or day number of year variation does not have good input data for the entire African region. As presented previously, this might be the reason for the shortfall in NN TEC model to capture the EIA feature in some cases. In order to have fairly adequate data, we did not apply restriction to the horizontal smear. Therefore, in a day, there were about 80 observations as shown with red stars in Figure above. It is clear that the ~80 COSMIC TEC data points in a day are still far less compared to 9,216 data points needed to fill all the grid cells in a day. This problem was partly solved by

adopting appropriate data binning criteria. For example, instead of binning data according to year, we binned data according to only three different solar flux levels (as in Mungufeni et al, (2019), *Characterization of Total Electron Content over African region using Radio Occultation observations of COSMIC satellites*, Adv in Space Res 65, 19 – 29).

We established that the COSMIC TEC data values with smear > 1500 km do not introduce alarming errors. This was done by analyzing COSMIC TEC data which were coincident with TEC observed by ionosonde stations at Hermanus, Grahamstown, and Louisvale. The observations of the year 2013 were considered. Table below presents the root mean squared error between (i) ionosonde and COSMIC TEC without limiting the horizontal smear, and (ii) ionosonde and COSMIC TEC with horizontal smear limited to 1500 km.

Station	Smear < 1500 km		No limitation	
	Number of observations	RMSE (TECU)	Number of observations	RMSE (TECU)
Hermanus	38	1.838	65	2.256
Grahamstown	34	6.479	73	7.923
Louisvale	42	2.765	91	3.252

The table shows that the RMSE for the two cases over a particular ionosonde station are not grossly different. Based on these results, trading off accuracy may not be costly compared to trading off adequate need of data. Therefore, we decided not to impose any restriction on the horizontal smear. Although the RMSE appear to be smaller when

the smear < 1500 km, some of the data points that were subjected to this restriction are also far from the linear least squares fitting line. See blue stars in Figure below.

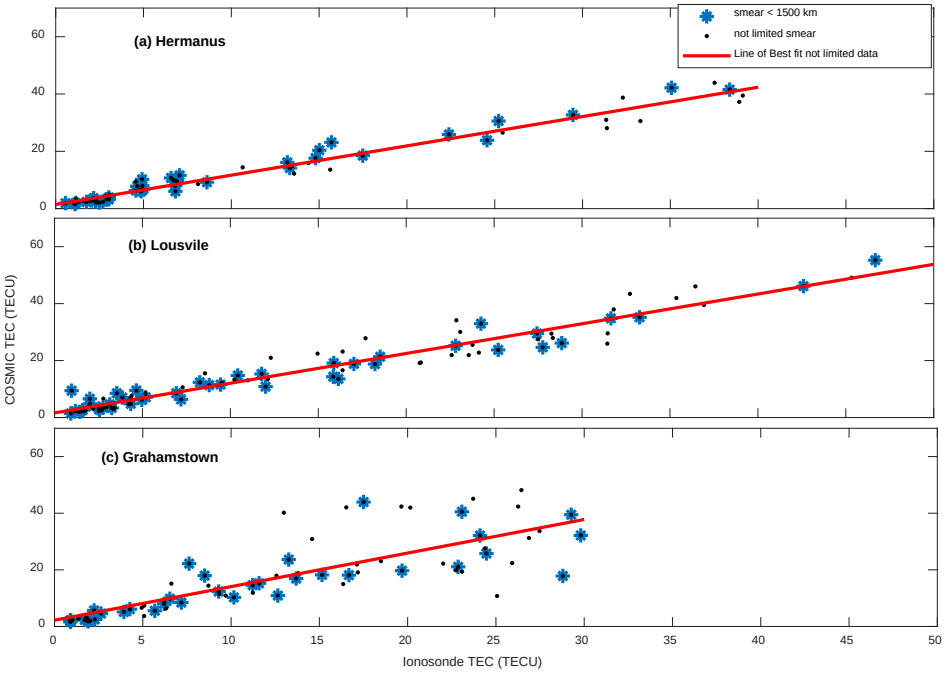

Comment:

I strongly suggest to compare the output of their model with ionospheric TEC (up to 700 km) from all over four stations Digisonde stations over South Africa https://spaceweather.sansa.org.za/products-andservices/current-conditions/ionograms. This will provide a much more realistic comparison test to their model

Response:

The suggested idea has been implemented in pages 19 - 21.

We illustrate in Figure below with magenta lines the diurnal patterns of TEC measured by ionosonde stations at Hermanus (panels in column (i)), Grahamstown (panels in column (ii)) and Louisvale (panels in column (iii)). The corresponding TEC generated by our spline technique model (spline), Nequick 2, and IRI-2016 are superimposed with red, green and blue lines, respectively. We need to mention that during computation of TEC using NeQuick 2 and IRI-2016, the height was limited to the approximate altitude of the COSMIC satellites (800 km). The panels in rows (a) - (c) show TEC on day of year 170 (June), 260 (September), and 350 (December), respectively. All these three days of the

year 2013 were geomagnetically quiet. Preliminarily, figure below appears to reveal that IRI-2016 either overestimates (December) or underestimates (June and September) the TEC measured by the ionosonde stations. On the other hand, our spline model and NeQuick 2 seem to depict good correspondence between the observed and the modeled TEC. It can also be seen from figure below that over a particular station, the shape of curves on different days representing TEC generated by the IRI-2016 and NeQuick 2 models are similar. This is expected since these two models were meant to reproduce monthly median values of the ionosphere. This means that our model, based on spline functions may capture better the day-to-day variability of the ionosphere.

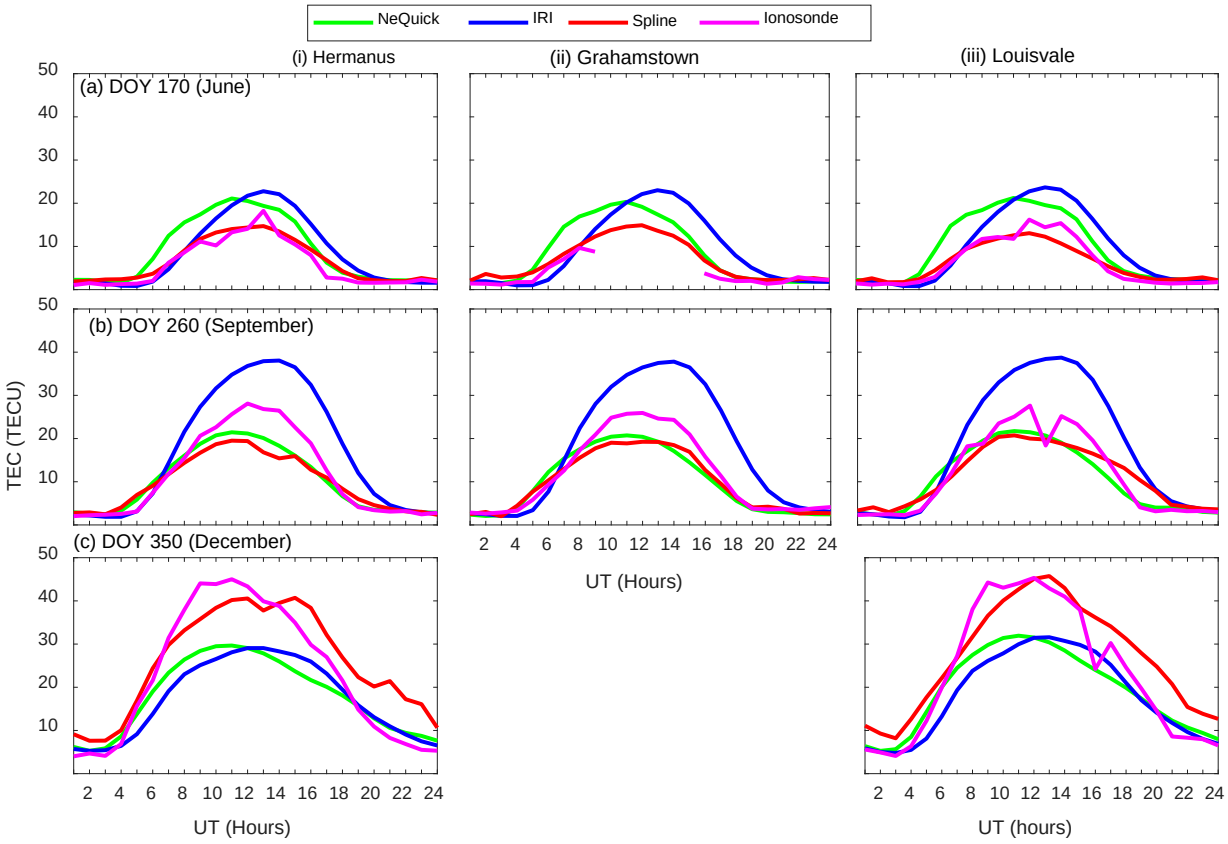

We generated such data plotted in the above figure for the entire year 2013 and then perform statistical analysis of the differences between the observed and the model TEC

data. Table below presents in columns 3 the correlation coefficients, r for the correlations between modeled and ionosonde TEC. Moreover, the table presents the RMSE when the ionosonde TEC was estimated using the models listed in column 2. The number of observations, n over each station that were used to determine, r and RMSE are put in brackets below the station name.

Ionosonde Station /number of observations	Model	r	RMSE (TECU)
Hermanus (n = 5,110)	Spline	0.92	4.64
	IRI-2016	0.86	5.45
	NeQuick 2	0.92	4.10
Grahamstown (n = 4,450)	Spline	0.88	5.56
	IRI-2016	0.82	6.29
	NeQuick 2	0.86	5.27
Louisville (n = 4,543)	Spline	0.94	3.82
	IRI-2016	0.87	5.62
	NeQuick 2	0.94	3.73

It can be seen from the Table that the r values associated with NeQuick 2 and spline based model are consistently better when compared with that of IRI-2016. Moreover, the RMSE values associated with IRI-2016 are the highest in all the cases. These two observations indicate that compared to spline and NeQuick 2, IRI-2016 poorly estimates TEC at the locations of the ionosondes. The RMSE values associated with NeQuick 2 are always slightly lower than that of spline, while the r values associated with spline are mostly comparable or slightly higher than that of NeQuick 2. These discussions demonstrate that our spline model generates TEC values consistently with that observed by ionosondes. This implies that equivalent TEC measured by ionosondes over locations which do not have ionosonde stations can be predicted fairly well using our model.

Responses to Reviewer #2

Comment:

The manuscript presents an empirical model describing ionosphere total electron content over African region. Authors use experimental TEC data obtained using dual frequency GNSS RO receivers onboard of COSMIC satellites to construct the model. They validate the model using same type of data that was used to construct the model but for a different period.

Response:

In addition to using the same type of data for validating our model, we have used TEC measured by ionosonde stations over South Africa. See pages 19 – 21 in the revised manuscript. Also see the preceding response to last comment of reviewer #1.

Comment:

General impression is that the present work has no contribution to the current understanding of the low latitude ionospheric physics/modelling. The work brings a little science and the newly created model could hardly be used in any real-life application. Authors are making too many assumptions and mistakes, sometimes trying to deliberately present performance results better than they are. Moreover, the performance of the model has not been compared to any other well-known model, leaving a room for doubts. Therefore, I recommend the manuscript (in its present form) is **rejected**. At the same time, the work might be improved and worth publication after substantial modifications. Please find below a list of critical issues along with possible improvements/corrections for a potential future re-submission.

Response:

Since all the comments by the editor and reviewers have been addressed appropriately, we do not expect a decision to reject our manuscript.

Comment:

P.1 L.27: Replace "good" with "applied". Otherwise, provide a proof of the model "goodness"

Response:

The suggestion has been implemented on page 1, line 22.

Comment:

P.2. L.35-38: Not all GNSS systems support ionospheric corrections. E.g. GLONASS does not broadcast any ionospheric model parameters. Correct the sentence accordingly.

Response:

The suggested correction can be seen on page 2, line 7 - 8.

Comment:

P.2 L.40: Provide a reference to the original description of Klobuchar model: *"Klobuchar JA (1987) Ionospheric time-delay algorithm for single frequency GPS users. IEEE Trans Aerosp Electron Syst 23(3):325–331. https://doi.org/10.1109/TAES.1987.310829"*

Response:

The suggested reference has been added on page 2, line 11 and page 28, lines 1 - 3.

Comment:

P.2 L.41-42: NeQuick G model is based on the NeQuick model, but not NeQuick 2. Correct the statement and the reference accordingly, e.g. *"EC (2016) European GNSS (Galileo) Open Service—Ionospheric correction algorithm for Galileo single frequency users, Issue 1.2, Sept. 2016, European Commission"*

Response:

The suggested correction can be seen on page 2, lines 12 - 15.

Comment:

P.2. L.42: Change “The NeQuick is” to “The NeQuick and its subsequent modifications (NeQuick G and NeQuick 2) are”

Response:

The suggestion has been implemented on page 2, lines 15 - 16.

Comment:

P.2 L.53: IRI model does not provide information about “electron and ion velocities”. It only provides information about equatorial vertical ion drift. Correct the sentence accordingly.

Response:

The sentence has been corrected as below.

“ …….parameters (such as electron density, electron and ion temperatures, and equatorial vertical ion drift), ……”

In the revised manuscript, it appears as seen on page 2, lines 26 - 27.

Comment:

P.2 L.55-56: Change “The model is primarily” to “IRI is an empirical model primarily”

Response:

The suggestion has been implemented as seen on page 3, line 1.

Comment:

P.3 L.74: Change “GIM” to “global ionosphere model”, as GIM is already defined to be Global Ionosphere Map.

Response:

The suggestion has been implemented in page 3, line 19.

Comment:

P.3 L.76: Change “GIM model” to “global ionosphere model”

Response:

The suggestion has been implemented in page 3, line 21.

Comment:

P.3 L.80-82: The high values of RMS in low latitude region provided by CODE is,

primarily, due to the inability of the selected model function (spherical harmonics) to describe ionospheric structure in low latitude. Modify the sentence accordingly.

Response:

We based on Fig below (obtained from Najman, P. and Kos, T.: Performance Analysis of Empirical Ionosphere Models by Comparison with CODE Vertical TEC Maps, Chapter 13, in: Mitigation of Ionospheric Threats to GNSS: an Appraisal of the Scientific and Technological Outputs of the TRANSMIT Project, InTech Open Science publications, pp. 162 - 178, doi:10.5772/58774, 2014) to make the statement, “This could be due to the poor distribution of IGS tracking stations over Africa and anomalies in the ionosphere related to the geographic and geomagnetic location”.

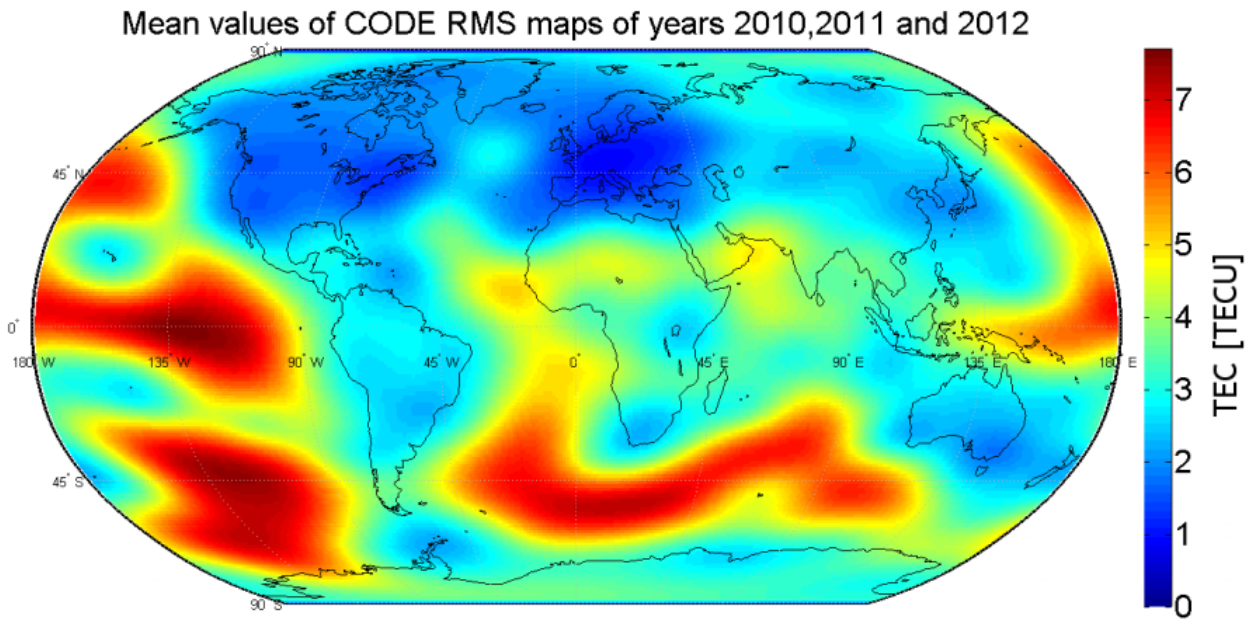

Indeed, figure above shows high RMS values over the oceans and land masses that have few/no ground based GPS receivers. This situation typically exists around and over the African continent.

Since figure above does not strictly show high values of RMS over all low latitude regions where EIA exists, we removed EIA as a reason for the high RMS values over

Africa. We have included “inability of spherical harmonics function ….” on page 3, lines 26 – 27.

Comment:

P.3 L.84: Change “the GIM model” to “global models”

Response:

The suggestion has been implemented in page 3, line 29.

Comment:

P.4 L.115: Author use TEC integrated up to COSMIC satellite heights (800 km) to construct the model (*“integration being done up to the altitudes of the COSMIC satellites”*). However, the topside TEC values (according to numerous studies, e.g. by Bilitza 2009, Yizengaw 2008 etc.) can reach from 10% to 80% of the total electron content (from ground to GNSS satellite heights). This fact significantly reduces the scientific value and application of the developed model. Essentially, the model is useless for GNSS applications.

Response:

This comment is similar to that of reviewer #1 to which we already responded in this document on pages 4 - 5. In the revised manuscript, we justified lack of inclusion of plasmaspheric TEC in COSMIC RO TEC in page 5, lines 12 - 29 and page 6, lines 1 - 5. The significance of the current study has been provided in page 6, lines 2 – 5 and page 1, lines 27 - 31.

The highlights of justifications of lack of inclusion of plasmaspheric TEC and significance of this study are as follows.

In order to get integrated electron density approximately up to the altitudes of GPS satellites, Okoh et al., (2019) used neural networks to learn the relationship between coincident TEC measurements done by ground based GPS receivers and COSMIC RO. They showed that the ratio between TEC data from the two sources vary spatially. This observation implies that the neural networks may not learn very well the relationship between TEC measured by ground-based GPS receivers and COSMIC RO over locations which do not have the former data set during the entire study period. As

shown previously in response to reviewer #1, there were large spatial coverage's that do not have ground based GPS receivers. Due to such problems, we used only COSMIC TEC without any adjustments.

We examined the available differences between coincident COSMIC RO TEC and ground based GPS TEC. Concerning the region under study, the upper quartile of the differences between coincident COSMIC RO TEC and ground based GPS TEC could reach ~11 TECU (Mungufeni et al, (2019), *Characterization of Total Electron Content over African region using Radio Occultation observations of COSMIC satellites*, Adv in Space Res 65, 19 – 29). Since the upper quartiles of the differences can reach up to ~11 TECU, the median/mean values might obviously be much lower than this value. This might be the reason for observing most of the well known ionospheric TEC features over the African region when the COSMIC RO TEC were appropriately binned in the above reference. The ionospheric features being referred to include; (i) occurrence of minimum and maximum TEC during 0:00–08:00 LT and 12:00–16:00 LT respectively, (ii) occurrence of secondary TEC enhancement (maximum) during 16:00–20:00 LT, (iii) lowest TEC values being observed in June solstice and highest TEC values observed in March equinox, (iv) TEC values increase as solar activity changes from low to high, (v) mid latitude TEC values are lower than those of low latitude regions, and (vi) occurrence of equatorial ionization anomaly.

Therefore, the current model was built with the aim of reproducing these known ionospheric features. Such endeavors are important for educational purposes. Moreover we illustrated in a previous response that our model generates TEC values consistently with that observed by ionosondes. This implies that equivalent TEC measured by ionosondes over locations which do not have ionosondes can be predicted fairly well using our model.

Comment:

P.5 L.124-126: This statement "*Since the magnitudes of the TEC obtained from COSMIC occultation 124 measurements are close to ground based GNSS TEC*", is not consistent with the previous statement and studies by Mungufeni et al. 2019. Where

they show that, depending on the location, the RMS error can vary from 2 to 8 TECU and error distribution plots show values from -24 to 20 TECU. Such large errors cannot be considered "*close to ground-based GNSS TEC*". Authors, at least, are expected to provide information about relative TEC errors (in %, rather than TECU) to claim that errors can be tolerated (if so).

Response:

In addition to the quoted sentence which appears in the revised manuscript on page 5, lines 23 – 27, on page 5, lines 27 – 29 and page 6, lines 1 - 5, we have added the following information.

Since the upper quartiles of the differences can reach up to ~11 TECU, the median/mean values might obviously be much lower than this value. This might be the reason for observing most of the well known ionospheric TEC features over the African region when the COSMIC RO TEC were appropriately binned in the above reference. The ionospheric features being referred to include; (i) occurrence of minimum and maximum TEC during 0:00–08:00 LT and 12:00–16:00 LT respectively, (ii) occurrence of secondary TEC enhancement (maximum) during 16:00–20:00 LT, (iii) lowest TEC values being observed in June solstice and highest TEC values observed in March equinox, (iv) TEC values increase as solar activity changes from low to high, (v) mid latitude TEC values are lower than those of low latitude regions, and (vi) occurrence of equatorial ionization anomaly.

Therefore, the current model was built with the aim of reproducing these known ionospheric features. Such endeavors are important for educational purposes. Moreover we illustrated in a previous response that our model generates TEC values consistently with that observed by ionosondes. This implies that equivalent TEC measured by ionosondes over locations which do not have ionosondes can be predicted fairly well using our model.

Comment:

P.6 L.150: The title of the reference Emmert et al. 2010 is incorrect: *Emmert, J. T., Richmond, A. D., and Drob, D. P.: Statistical analysis of the correlation 412 between the equatorial electrojet and the occurrence of the equatorial ionisation 413 anomaly over the East African sector, J. Geophys. Res., 15; A08322; 414 doi:10.1029/2010JA015326, 2010.*

Response:

The correction has been made. See page 27, lines 2 – 4.

Comment:

P.6 L.157-167: The selected spatial resolution of 15º in longitude and 5-8º in latitude is too coarse to describe the ionosphere reasonably, especially for the low latitude region, where TEC is changing dramatically from the crest down/up to two peaks of EIA. E.g. GIM maps (the source of the data for most of the empirical models discussed by the authors in the introductions section) use at least 5º by 2.5º resolution (lon and lat). Moreover, 15º in longitude corresponds to 1 hour in LT. Gradients in TEC as a function of LT during sunrise and sunset hours may reach tens of TECU per hour (e.g. Mungufeni et al. 2019, Fig. 2). Therefore, such coarse spatial resolution in longitude will lead to big errors in the model description.

Response:

We have now developed the model using data binned in grids with longitude range of 5º and latitude range of 3º. See page 7, lines 10 – 12 and page 12, lines 4 - 6. This fairly high resolution allowed us to observe the EIA features as seen in Figure 7 on page 24.

Comment:

P.6 L.170: The whole solar cycle 24 has relatively low solar activity level compared to the two previous ones. Nevertheless, even if we look only at the 24th solar cycle, 2011 and 2016 could hardly be attributed as years of high solar activity level. Please, modify the statement accordingly (e.g. as it is done on P.7 L.182).

Response:

The sentence has been modified as shown on page 7, line 1.

Comment:

P.7 L.189: Please clarify, how 36 solar flux bins were obtained. From the description, it is only 3 solar flux ranges and 12 months, that gives 36 (3x12). But when listing by a variable, only number 3 has to be specified, as it is done, for example with the rest of the variable (hour, lat and lon). Indeed, if we take 60,480 TEC values indicated in L.189, this number can be obtained by multiplying 5x14x3x12x24, but not 5x14x36x12x24.

Response:

In each of the 3 solar flux ranges, there are 12 nodes, corresponding to the months in a year (see table 2). This results into the 36 solar flux nodes. The listing in equation 1 on page 11 has reflected this. Moreover the longitude and latitude nodes have changed to 16 and 24, respectively.

Comment:

P.8 L.205: According to the definition of cubic spline, it is a spline constructed of piecewise third order polynomials, meaning none of the B splines used in the model were cubic (order 2 and 4). Change the "cubic B spline" into "B spline of different orders" throughout the text and abstract.

Response:

The suggestion has been implemented. See page 11, lines 24 - 25; page 1, line 17; and page 25, line 9.

Comment:

P.9 L.218-220: Consider changing this sentence to something like "In order to assess the ability of the model to describe the data used to construct the model, modelled data were compared to the experimental one. The results of the self-consistency check are presented in Figure 1."

Response:

This suggestion has been implemented in the manuscript on page 12, lines 10 – 12.

Comment:

P.9 L.228-229: It is surprising that the authors compare the results of the climatological model (i.e. model where input data were averaged over time, e.g. one month) with GIM map for a single day of that month. Such a comparison is not correct. On top of that, by

looking at TEC maps obtained from COSMIC and later by B spline model (columns 2 and 1), one can hardly see any separation between the peaks of the EIA, that can, taking into account averaging in all the bins (e.g. lat and lon) performed by authors, hardly be comprehended.

Response:

Now the GIM-TEC panel has been removed. See figure 1 in page 13 (see also figure below). After reducing the spatial resolution of the data, figure 1 showed distinct two crests and a trough, particularly before 18:00 LT. After this time, when the zonal electric field reverses westwards, upward plasma drift (responsible for EIA formation) is altered, leading to no separation of crests.

Comment:

P.9 L.231-232: By looking at the color plots, a reader can hardly assess the performance of the model. It is suggested, in addition to the plots, to present/discuss the results of the mismodelling in terms of a bias and RMS of the error.

Response:

Third column panels in Figure 1 on page 13 (see also figure below) present the error map which shows error values < 0.1 TECU.

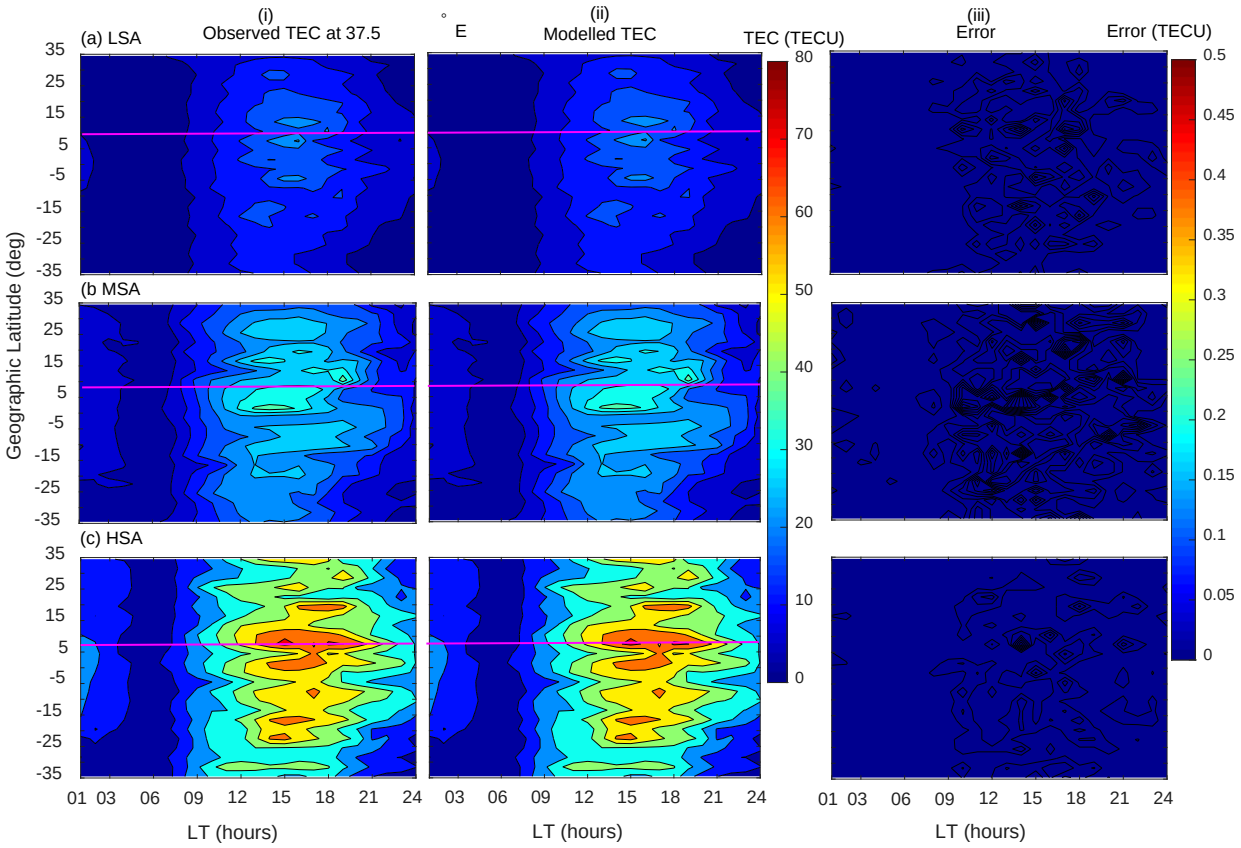

These really small magnitudes of the errors may not require statistical analysis to demonstrate that the errors can be tolerated.

Comment:

P.10 L.250-252: From Fig 1 it cannot be clearly understood the secondary maximum if any, especially at -20 lat. Please, if you discuss a feature, try demonstrating it clearly to the reader. A separate figure, or at least, a dashed line at -20 and 4 in Fig 1 is needed to support the statement.

Response:

The current figure 1 on page 13 (also see above figure) has a good mark for pointing at the two peaks of diurnal TEC. In revised manuscript, see text on page 13, lines 14 – 15. The mark used to point at the two peaks is the magenta line on panels in row (c). We computed at lon 37.5^{o} N, the corresponding geographic latitude of the magnetic equator as ~9^{o} N. Figure above shows that the trough is not centered on the magnetic equator. Past studies (e.g Mungufeni et al., (2018): Statistical analysis of the correlation between the equatorial electrojet and the occurrence of the equatorial ionization anomaly over

the East African sector, Ann. Geophys., 36, pp. 841 – 853, 2018) show that the EIA trough is not exactly centered at the magnetic equator, particularly at the location of figure above.

Comment:

P.11 L.269-270: In row (b), Fig 1, none of the panel show peaks of the EIA. There is no clear separation of the crest and peaks of EIA. Nor in panels b1/b2 neither in b3. Modify the sentence accordingly.

Response:

This comment about separation of EIA crests was previously raised and we already responded.

Comment:

P.277-279: The structure of the crest might differ based on various factors (including level of the geomagnetic disturbance). However, when taken as an average, a clear 2 peak structure is present in low latitudes, representing EIA.

Response:

Based on the remark in the comment we have removed the statement about observation of several crests and discussions associated with it.

Comment:

P.12 L.298-299: The science question in this case is not how to model the observed data, but how to explain the data. What is the physical explanation for the absence of the EIA structure (two peaks and the crest) in TEC values calculated from the ground up to COSMIC satellite heights (~800km). And whether this phenomena is not a limitation of the technique applied to calculate TEC. Namely, TEC computed by integrating electron density profile, that by itself is a product of RO inversion, is subject to big errors, especially in places where big horizontal gradients exist (read, e.g. M.M Shaikh et al., Implementation of Ionospheric Asymmetry Index in TRANSMIT Prototype, DOI: 10.5772/58551). Without understanding the reasons of the observed behavior all the modeling efforts are meaningless.

Response:

In the paragraph under question, we mentioned asymmetry of EIA feature and occurrence of secondary peak in TEC over Africa. We further mentioned that these features can be seen in the data we used to develop our model. Therefore, our model emulates these features. We would like to mention that these two features have been well explained in the manuscript (see page 13, lines 12 – 18, page 14, lines 1 – 9; and page 16, lines 3 – 9.

The reviewer's phrase, "absence of the EIA structure (two peaks and the crest) in TEC values calculated from the ground up to COSMIC satellite heights (~800km)" did not exist in our manuscript. This makes it difficult for us to understand the point the reviewer would like to make. Anyway, we guess that the reviewer is talking about the absence of asymmetry of EIA feature in GIM-TEC. In case this is correct, as stated before, we removed presentation and discussions of comparison of our model with GIM-TEC.

Comment:

P.13 L.313: One cannot see the "perfect match" of the observed and modelled data just by looking at the plots. At least a third row in form of difference map (error map) has to be presented to visually assess the error level. Moreover, statistical results (e.g. RMS and bias of the error) must be presented in order to make such a bold conclusion.

Response:

We have provided in the third column panels of figure below (see in revised manuscript Figure 1 on page 13) the error levels between the observed and the measured data.

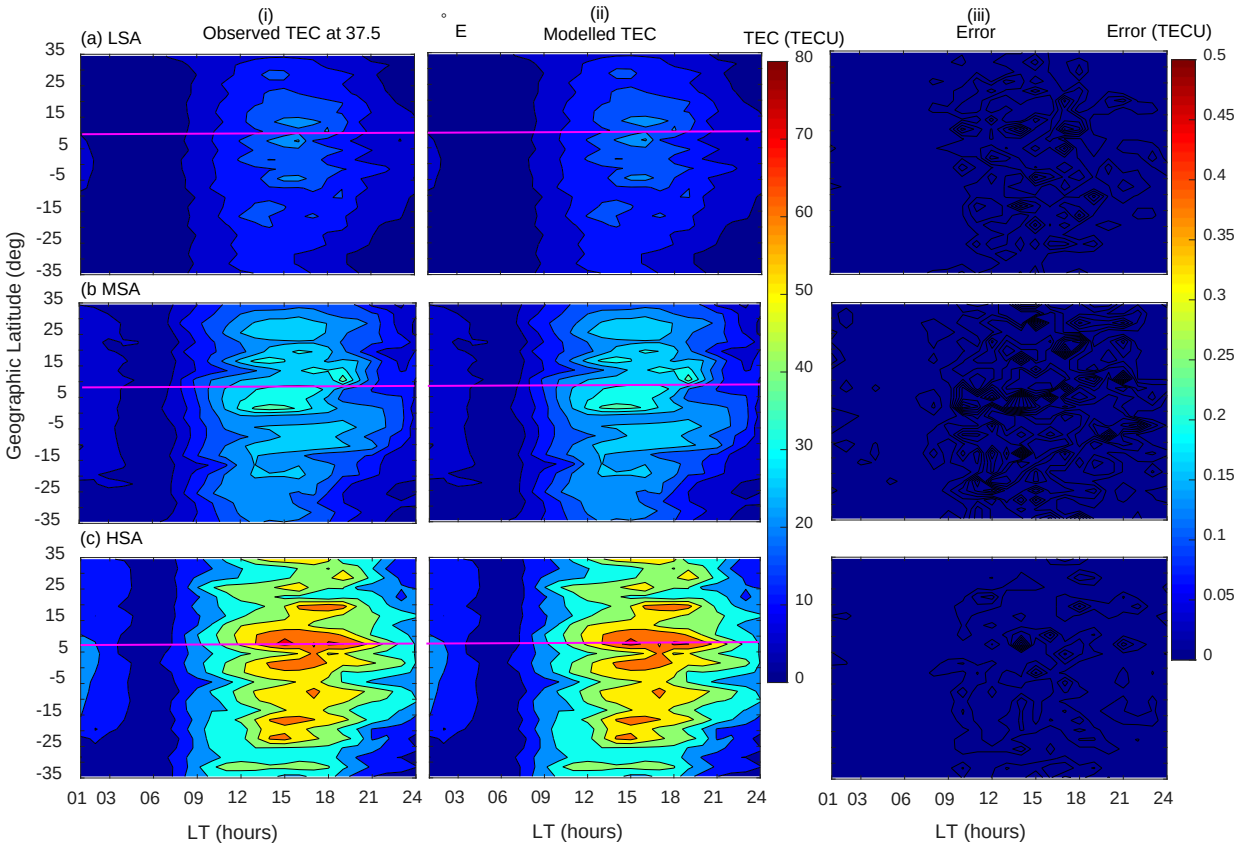

The error maps show values < 0.1 TECU (see the color bar). This means as expected, the observed and the modeled data almost match perfectly. Without performing statistical analysis, the fact that all error values are < 0.1 TECU gives the confidence of making the conclusion that the observed and modeled data almost match perfectly. Performing statistical analysis would be necessary if some error values were fairly high.

Comment:

P.13 L.312-324: Authors do not discuss at all the TEC behavior observed in September at lat ~ -20, where its diurnal variation has a maximum during local night hours (21-03 LT). This maximum seems to exceed any other TEC values on this plot (row c, column 1 and 2) and looks like an error in the data processing. Such behavior seems to have no physical explanation.

Response:

After carefully analyzing the data again the feature mentioned in the comment was no longer seen. In the revised manuscript, see figure 2 on page 15. The figure is reproduced below.

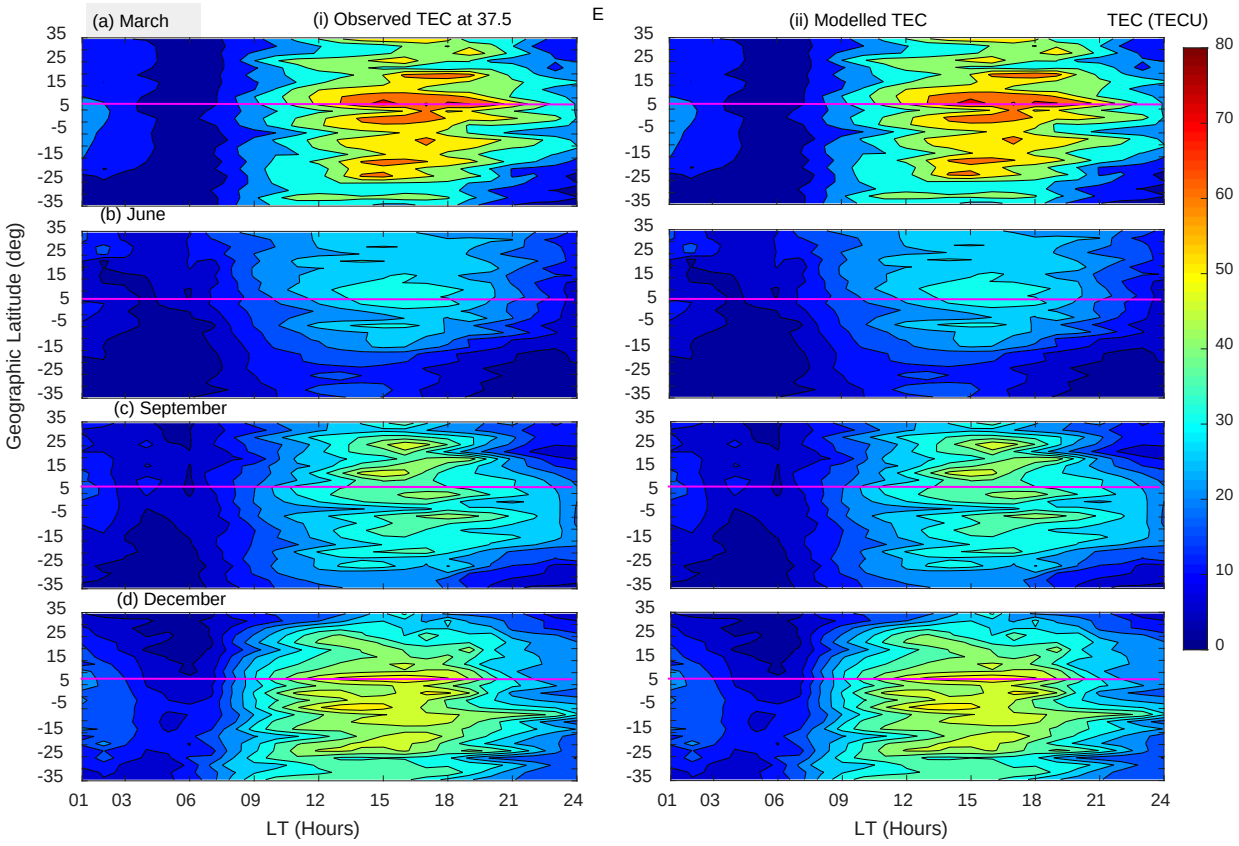

Comment:

P.14 Section 5: The authors fail to explain why they need yet another TEC model. Unless the performance of the newly created model is compared to existing models and it is demonstrated that its any better than the rest of the models present on the "ionosphere model market" (e.g. IRI, NeQuick, NTCM etc.), there is very little value in the study (both scientifically and application-wise).

Response:

As seen in our previous responses to reviewer #1 in this document on page 13, we compared our model with the existing models such as IRI, NeQuick, and AfriTEC (Okoh et al. 2019). Also see in the revised manuscript sections 5.2 and 5.3. In page 20 of this document, we had provided the scientific significance of this study. On page 19 of this

document, we provided the page and line numbers in the revised manuscript where the scientific significance of this study can be seen.

Comment:

P.15 L.350-353: Figure 4 does not show the full picture of the error distribution. It is clearly cut at -14 and 14 TECU. Iif one looks at Figure 3, errors in TEC can easily reach +-20 TECU (just draw a vertical line at any value of Observed TEC, e.g. at 30 TECU). It looks like the authors deliberately try to improve the results of their model performance.

Response:

Actually, we should have not indicated ±16 on the horizontal axis. Moreover, we should have indicated on the horizontal axis < -14 (instead of merely -14) and > 14 (instead of merely 14). The total number of errors with values in the range of -14 – 14 TECU was 16858 (97.4 %), while the number of errors with values outside this range was 454 (2.6 %). By comparing these two percentages, it can be deduced that the number of errors with values outside the range of -14 – 14 TECU was insignificant. After implementing the above changes, Figure 4 would appear as below. In the revised manuscript, see on page 18. We have also superimposed the percentages of the different error levels. This is in accordance with the previous comment of the reviewer.

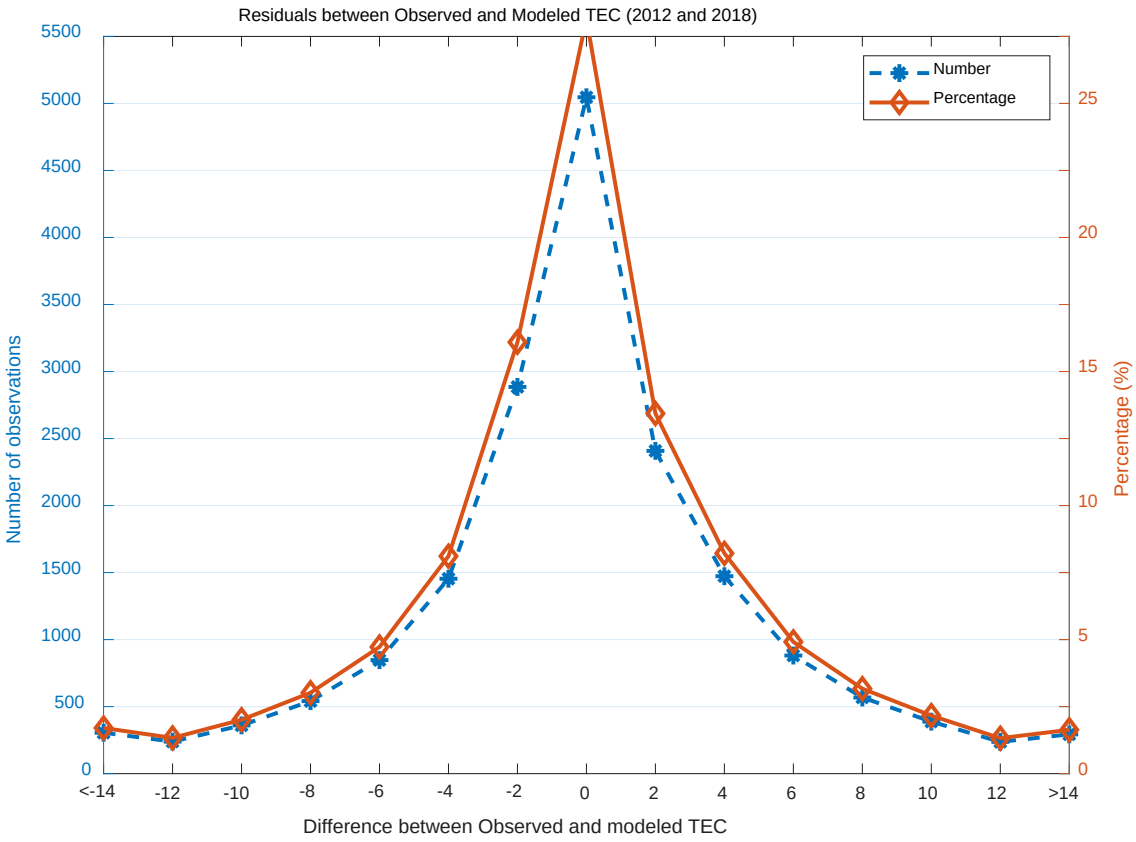

Minor/Typo comments:

Comment: P.1 L.17: Change “derived” to “obtained”

Response: Done as seen on page 1, line 13

Comment: P.1 L.19: Change “Geomagnetically quiet time (Kp < 3 and Dst > -20 nT) data during the years” to “Data during geomagnetically quiet time (Kp < 3 and Dst > -20 nT) for the years”

Response: Done as seen on page 1, line 15 - 16.

Comment: P.1 L.22 Change “to obtain the model” to “to obtain model coefficients”

Response: Done as seen on page 1, line 18.

Comment: P.1 L.26 Change “COSMIC TEC” to “COSMIC RO TEC”

Response: The sentence associated with the phrase was stating that our model is the first over the entire African region. After the publication of Okoh et al., (2019), this became invalid. Therefore, the sentence that contained the phrase in the comment was removed.

Comment: P.2 L.31: Change “using Global Navigation Satellite Systems” to “in Global Navigation Satellite Systems”

Response: Done as seen page 2, line 2 - 3.

Comment: P.2 L.30 Change “during day” to “during the day”

Response: The corrected can be seen on page 2, line 11.

Comment: P.2. L.49: Space is missing between “European Geostationary”

Response: See page 2, line 23.

Comment: P.2 L.50: Change “GPS And Geo-Augmented Navigation” to “GPS-aided Geo Augmented Navigation”

Response: see page 2, line 24.

Comment: P.3 L.63: Space is missing in “analysis centers”

Response: See page 3, line 11 - 12.

Comment: P.3 L.64: Space is missing in “using the”

Response: See page 3, line 10.

Comment: P.3 L.64: Change “Global Ionospheric TEC data Map (GIM)” to “Global Ionosphere Maps (GIMs) containing vertical TEC data”

Response: See page 3, line 9.

Comment: P.3 L.66: Change “Global Ionospheric TEC data Maps (GIMs)” to “GIMs”. It has been defined two lines above.

Response: See page 3, line 11.

Comment: P.3 L.70: Space is missing in “the average”

Response: See page 3, line 14 - 15.

Comment: P.3 L.71: Space is missing in “by CODE”

Response: See page 3, line 16.

Comment: P.3 L.76: Space is missing in “constructed a”

Response: See page 3, line 21.

Comment: P.3 L.77: Space is missing in ”GPS radio”

Response: Page 3, line 22.

Comment: P.3 L.82: Space is missing in “related to”

Response: The phrase was contained in a sentence which stated that the high RMSE values were due to EIA. After observing that some EIA regions depicted low RMSE values, the statement became invalid. Therefore, the sentence which contained the phrase in the comment was removed.

Comment: P.4 L.87: Change “localized ionospheric structure” to “localized ionospheric structures”

Response: See page 4, lines 3 – 4.

Comment: P.4 L.88: Change “on a global scale model” to “in global models”

Response: See page 4, line 4.

Comment:P.5 L.140: Space is missing in “during geomagnetically”

Response: See page 6, lines 18 - 19 .

Comment:P.6 L.147: Change “solar activity” to “solar activity level”

Response: See page 6, line 26.

Comment:P.6 L.164: Remove “15” in “reduced 15 to 5”

Response: Since the spatial resolutions were changed, the phrase in the comment was removed.

Comment:P.7 L.181 Space is missing in “the F10.7”

Response: See page 9, line 1.

Comment:P.9 L.223: Change “Global Ionosphere Map (GIM) TEC (GIM-TEC)” to “GIM TEC”, as it was defined earlier, remove “Center for Orbit Determination in Europe” – it was defined earlier

Response: Since the reviewer did not recommend comparison of our model with the CODE GIM, the phrase in the comment was removed.

Comment:P.9 L.225-226: Remove “The daily GIM-TEC values are derived using the GNSS data collected from over 200 tracking stations of IGS and other institutions”, as this information was given earlier in the text

Response: For the same reason given in the preceding response, the phrase in the comment was removed.

Comment:P.10 L.238: Space is missing in “in turn”

Response: See page 12, line 27.

Comment:P.14 L.336: Change “;” to “:”

Response: See page 16, line 22.

Comment: P.14 L.337: Space is missing in “root mean squared”

Response: See page 16, line 23.

Comment: P.17 L.373: Change “:” to “.” In “0.93”

Response: See page 25, line 14.

Modeling Total Electron Content derived from radio occultation measurements by COSMIC satellites over the African region

Patrick Mungufeni[1], Sripathi Samireddipalle[2], Yenca Migoya-Orué[3], and Yong Ha Kim[1]

[1]Department of Astronomy and Space Science, Chungnam National University, Daejeon, South Korea
[2]Indian Institute of Geomagnetism, New Panvel, India
[3]The Abdus Salam International Centre for Theoretical Physics (ICTP) T/ICT4D

Abstract

This study developed a model of Total Electron Content (TEC) over the African region. The TEC data were obtained from radio occultation measurements done by the Constellation Observing System for Meteorology, Ionosphere, and Climate (COSMIC) satellites. Data during geomagnetically quiet time (Kp < 3 and *Dst* > -20 nT) for the years 2008 - 2011, and 2013 – 2017 were binned according to local time, seasons, solar flux level, geographic longitude and latitude. B splines were fitted to the binned data to obtain model coefficients. The model was validated using actual COSMIC TEC data of the years 2012 and 2018. The validation exercise revealed that, approximation of observed TEC data by our model produces root mean squared error of 5.02 TECU. Moreover, the modeled TEC data correlated highly with the observed TEC data (r = 0.93). Due to the extensive input data and the applied modeling technique, we were able to reproduce the well-known TEC features such as local time, seasonal, solar activity cycle, and spatial variations over the African region. Further validation of our model using TEC measured by ionosonde stations over South Africa at Hermanus, Grahamstown and Louisville revealed r values > 0.92 and RMSE < 5.56 TECU. These validation results imply that our model can estimate fairly well TEC that would be measured by ionosondes over locations which do not have the instrument. Another importance of this study is the fact that it has shown the potential of using basis spline functions for modeling ionospheric parameters such as TEC over the entire African region.

1. Introduction

Among the error sources that affect the positioning in Global Navigation Satellite Systems (GNSS) are the propagation medium related errors. In particular, the ionospheric refraction is the largest contributor of the user equivalent range error. This type of frequency dependent error can virtually be eliminated in dual frequency receivers by differential techniques (Hofmann-Wellenhof et al., 2007). For the case of single frequency receivers, some GNSS (e.g Global Positioning System (GPS) and Galileo) broadcast message includes the parameters of an ionospheric model which can be used to compute and correct the ionospheric effects (Guochang, 2007). For instance, the GPS uses the Klobuchar model which represents the zenith delay as a constant value at night and a half cosine function during the day (Klobuchar, 1987). In the framework of the European Galileo constellation, the NeQuick G based on NeQuick model has been proposed to be used for single frequency positioning (see Issue 1.2, September, 2016 of European Commission, titled, European GNSS (Galileo) Open Service - Ionospheric correction algorithm for Galileo single frequency users). The NeQuick and its subsequent modifications (NeQuick G and NeQuick 2) are a three-dimensional, time dependent ionospheric electron density model developed by the Aeronomy and Radio Propagation Laboratory (ARPL) of the Abdus Salam International Center for Theoretical Physics (ICTP) in Trieste, Italy and the Institute for Geophysics, Astrophysics and Meteorology of the University of Graz, Austria (Nava et al., 2008). In addition to using models to reduce ionospheric refraction errors, Space Based Augumentation Systems (SBAS) such as the Wide Area Augmentation System (WAAS), the European Geostationary Navigation Overlay Service (EGNOS), and the GPS-aided Geo Augmented Navigation (GAGAN) are also used (Hofmann-Wellenhof et al., 2007).

For the international standard specification of ionospheric parameters (such as electron density, electron and ion temperatures, and equatorial vertical ion drift), the Committee on Space Research (COSPAR) and the International Union of Radio Science (URSI) recommended the International Reference Ionosphere Model (IRI) (Bilitza, 2001). IRI is an empirical model primarily based on all available experimental data (ground and

space based) sources. However, theoretical considerations have been used in bridging data gaps and for internal consistency checks (Bilitza, 2001).

The ionospheric Total Electron Content (TEC) is one of the important descriptive physical quantities of the ionosphere (Rama Rao et al., 1997; Ercha et al., 2012). The GNSS measurements obtained from the global and regional networks of International GNSS Service (IGS) ground receivers have become a major source of TEC data. As one of the IGS analysis centers, Center for Orbit Determination in Europe (CODE) provides Global Ionosphere Maps (GIMs) containing vertical TEC data daily using the GNSS data collected from over 200 tracking stations of IGS and other institutions. Several studies have used GIMs from CODE and other IGS analysis centers such as the Jet Propulsion Laboratory (JPL) to construct TEC models (Jakowski et al. 2011a; Mukhtarov et al. 2013; Ercha et al. 2012; Sun et al., 2017). Jakowski et al. (2011a) proposed the Global Neustrelitz TEC Model (NTCM-GL) that describes the average TEC under quiet geomagnetic conditions. The NTCM-GL was developed using GIMs during 1998 - 2007 provided by CODE. A global background TEC model was also built using CODE GIMs by Mukhtarov et al. (2013). The model describes the climatological behavior of the ionosphere. The GIMs from JPL were used by Ercha et al. (2012) to construct a global ionosphere model using Empirical Orthogonal Function (EOF) analysis method. The Taiwan Ionosphere Group for Education and Research constructed a global ionosphere model from GNSS and the Constellation Observing System for Meteorology, Ionosphere, and Climate (COSMIC) GPS radio occultation (RO) observations (Sun et al., 2017). The map of all the averaged Root Mean Squared (RMS) error values of CODE GIMs during the years 2010 - 2012 presented by Najman and Kos (2014) showed high values over low latitude African regions. This could be due to the poor distribution of IGS tracking stations over Africa and inability of the spherical harmonics function used in GIM to describe ionospheric structure over low latitudes.

In addition to the existing GIMs discussed in the previous paragraph, regional TEC maps and models have also been constructed. In comparison with the global models, regional TEC models might have better accuracy over the particular region for which it

was constructed. Opperman (2008) stated that the higher time and spatial resolution imaging achievable with regional models permits the analysis of localized ionospheric structures and dynamics not observable in global models. Examples of studies that developed TEC models over some parts of Africa are the following. A neural network model of GNSS - vertical TEC (GNSS-VTEC) over Nigeria was developed by Okoh et al., (2016) using all available GNSS data from the Nigerian GNSS Permanent Network (NIGNET). An adjusted spherical harmonic-based TEC model was developed by Opperman, (2008) using a network of South African dual frequency GPS receivers. Habarulema et al. (2011) presented the Southern Africa TEC prediction (SATECP) model that was based on the Neural Network technique. The SATECP generates TEC predictions as function of input parameters, namely, local time, day number of the year, solar and magnetic activity levels, and the geographical location. A neural network based ionospheric model was developed using GPS-TEC data over the East African sector by Tebabal et al. (2019). Recently, Okoh et al., (2019) used neural network technique to develop TEC model over the entire African region. In addition to using TEC obtained by COSMIC RO technique, they used TEC measured by GPS receivers on ground.

Due to the lack of a dense network of ground-based GNSS receivers and poor coverage of COSMIC RO data over the African region, the TEC model over the entire African region presented by Okoh et al. (2019) sometimes failed to capture the equatorial ionization anomaly (EIA) over the region. This point has been illustrated with examples in sections 2 and 5. In this study, we applied data binning method to the COSMIC RO TEC data that allowed development of an improved TEC model over the region. Moreover, we demonstrate the potential of the basis spline functions to model TEC over the African region. In section 2, the data and methods of analysis that were used in the study are described. The details of the model proposed in this study are described in section 3. We present comparison between the observed and modeled TEC in section 4. The model validation and the conclusions are presented in sections 5 and 6, respectively.

2. The Data and methods

2.1 Data sources

In order to overcome the problem of lack of a dense network of ground based GNSS receivers over the African region, this study used TEC data obtained from RO measurements done by the COSMIC satellites. The integrated electron density (integration being done up to the altitudes of the COSMIC satellites) which is being referred to as TEC in this study can be obtained from ionPrf files which are processed at the COSMIC Data Analysis and Archive Centre (CDAAC)(http://cosmic-io.cosmic.ucar.edu/cdaac/index.html). The TEC for the individual occultation events were assigned to the geographic coordinates of NmF2 in the same file.

In order to obtain integrated electron density approximately up to the altitudes of GPS satellites, Okoh et al., (2019) used neural networks to learn the relationship between coincident TEC measurements done by ground based GPS receivers and COSMIC RO. They showed that the ratio between TEC data from the two sources vary spatially. This observation implies that the neural networks may not learn very well the relationship between TEC measured by ground-based GPS receivers and COSMIC RO over locations which do not have the former data set during the entire study period. As it can be seen in Figure 1 of Okoh et al. (2019), there were large spatial coverages that do not have ground based GPS receivers. Unlike what has been done in Okoh et al. (2019) and Mungufeni et al. (2019) in the current work we used only COSMIC TEC without any adjustments.

In this regard, an analysis of coincident ground-based GNSS TEC and TEC from COSMIC occultation data performed by Mungufeni et al. (2019) reveals that the upper quartile of the differences between the two data sets may reach up to ~11 TECU over the northern crest of the Equatorial Ionization Anomaly. Over the southern mid-latitude region, the differences were low (~4 TECU). Since the upper quartiles of the differences can reach up to ~11 TECU, the median/mean values in the worst cases might obviously be much lower than this value. This might be the reason for observing most of the well-

known ionospheric TEC features over the African region when the COSMIC RO TEC were appropriately binned as in Mungufeni et al. (2019). Therefore, this study used the TEC obtained from COSMIC occultation measurements to develop TEC model over the African region in order to reproduce these ionospheric features. Such endeavors are important for educational purposes.

During geomagnetic storms, the variations in zonal electric fields and composition of the neutral atmosphere contribute significantly to the occurrence of negative and positive ionospheric storm effects in the low latitude region (Rishbeth and Garriot, 1969; Buonsanto, 1999; Adewale et al., 2011). Therefore, since the ionosphere changes in a complex manner during geomagnetic storms, we only considered data on quiet days. The quiet geomagnetic days were identified by examining the 3 hourly Kp and Disturbance storm time (Dst) indices that were obtained from the World Data Center of Kyoto, Japan (http://swdcwww.kugi.kyoto-u.ac.jp/). A day was considered to be quiet if all the 8 Kp values in that day were ≤ 3. In addition to satisfying this condition, the hourly values of Dst in that day should also have values ≥ -20 nT. The two conditions were applied to ensure that both low and mid/sub-auroral latitude geomagnetic disturbances are detected by Dst and Kp indices, respectively. In future, we intend to use TEC data during disturbed geomagnetic conditions to construct a TEC model during geomagnetically disturbed conditions.

2.2 Methods of Data Analysis

The TEC data during the years 2008 - 2011 and 2013 - 2017 were used for developing the TEC model over the African region. Due to the adequate data needed to develop an empirical model, we only reserved the data of the years 2012 and 2018 for validation. The period considered in this study represents data of both low and high solar activity level in sunspot cycles 23 and 24. The data within geographic latitude and longitude ranges of -35 – 35^{o} and -20 – 60^{o}, respectively, were used to cover the African region. Table 1 presents the number of days per year when there were TEC data over the African region. Since there are many geomagnetically disturbed days in high (2012 -

2015) and medium (2011 and 2016) solar activity years, the number of days with data is also reduced in such years compared to low solar activity years (2008 - 2010, 2018).

Table 1: Distribution of number of days with data

Year	Number of days with data
2008	219
2009	293
2010	235
2011	174
2012	169
2013	185
2014	164
2015	128
2016	151
2017	154
2018	211

It would be good to bin the TEC data according to geomagnetic latitudes since many structural and dynamical features of the ionized and neutral upper atmosphere are strongly organized by the geomagnetic field (e.g. Emmert et al., 2010). This may be complicated since geomagnetic latitude lines are not usually straight. For convenience and simplicity, we binned the data based on geographic coordinates. In order to observe small scale ionospheric structures, small grid resolutions of 3 and 5 degrees in geographic latitude and longitude, respectively were used to bin the TEC data. These grid resolutions resulted into 24 and 16 latitudinal and longitudinal bins, respectively. Several studies (e.g Krankowski et al., 2011 and Mengist et al., 2019) that have used COSMIC data commonly consider measurements with horizontal smear > 1500 km prone to errors and they reject such measurements. We established that after applying this restriction, there were ~40 RO measurements per day during the year 2013 over our study area (not shown here). Based on the previous discussions, this value is far

less than the 9,216 (16 longitudinal, 24 latitudinal, and 24 local time) TEC data points required in all grid cells in a day. As stated in section 1, this poor amount of data to represent day of year TEC variation might be the reason for the failure of TEC model presented by Okoh et al. (2019) to capture in some cases the EIA over the African region. Another reason might be the discrepancy which arises due to some locations being represented by adjusted COSMIC RO TEC while others by the ground based GPS TEC data.

Since empirical modeling requires adequate data for the mathematical functions to capture the physics inherent in the data, this study did not reject COSMIC RO TEC measurements with horizontal smear > 1500 km. Although not presented here, we observed that the COSMIC TEC data values with smear > 1500 km did not introduce alarming errors. This observation was made when we analyzed COSMIC TEC data which were coincident with TEC observed by ionosonde stations over South Africa (see details in section 5.2) located at Hermanus, Grahamstown, and Louisvale. Interestingly, compared to measurements with horizontal smear > 1500 km, some measurements with horizontal smear < 1500 km were observed to be far from the linear least squares fitting line. Further analysis of COSMIC RO observations over our study area revealed that without restricting horizontal smear, there were ~80 RO measurements per day during the year 2013 (not shown here). Still this value is far less than the 9,216 TEC data values required to fill all spatial grid cells in a day. To partially solve this problem, instead of binning data according to year, we binned the data according to different solar flux levels as shown below.

For each spatial grid cell, the data were binned at 1-hour interval. TEC values within the bins were averaged to yield 1-hour resolution TEC data over the grids. TEC data for the different days were binned according to F10.7 flux of that day. The F10.7 flux indices were obtained from the Space Weather Prediction Center (SWPC) of the National Oceanic and Space Administration (NOAA) (http://www.swpc.noaa.gov/). The F10.7 flux ranges for low solar activity (LSA), medium solar activity (MSA), and high solar activity (HSA) were < 76, 76 - 108, and >108 sfu, respectively. The boundary values 76 and

108 sfu of the F10.7 flux ranges correspond to the 75*th* and 25*th* percentiles of all F10.7 flux values on the days in low (2008 - 2010, 2017 -2018) and high (2012 - 2015) solar activity years, respectively.

Table 2**:** Average monthly F10.7 flux values used in the study

Month	F10.7 flux (sfu)		
	LSA	MSA	HSA
January	71.10	83.94	140.65
February	71.14	87.06	126.23
March	69.81	85.40	130.98
April	71.02	86.09	130.46
May	70.29	90.59	123.80
June	69.51	89.91	118.73
July	68.09	88.14	128.92
August	67.45	85.46	114.53
September	69.20	86.34	122.98
October	70.06	81.88	131.50
November	71.66	82.40	142.95
December	70.82	82.97	142.72

The data within a specific solar flux bin were further binned based on months of a year. The average of the corresponding F10.7 flux of the days used to represent seasonal TEC were determined and used to capture the variation of TEC with solar flux. Table 2 presents the average F10.7 flux values that were determined in the months of a year. In summary, a total of 3,981,312 TEC data values were needed to exist in 16 longitudinal, 24 latitudinal, 36 solar flux, 12 monthly, and 24 hourly bins, in order to determine the model coefficients. However, from the data of the entire study period, only 121,447 bins

were filled with TEC data values. The remaining bins were filled by estimation following the procedures described in 3 steps below.

1. At a particular spatial grid cell, the diurnal TEC was divided into two local time sectors, namely, (i) 10:00 – 24:00 LT, and (ii) 0:00 – 10:00 LT. Sector (i) which is day time and before mid-night includes the time when daily and secondary TEC peaks are expected, while (ii) which is mostly at night is when TEC varies slowly. We need to mention that spline functions (De-Boor, 1978) were used to estimate missing TEC values. When slow variation of TEC was expected as in sector (ii), estimations were done when there were at least a few (>2) TEC data available. In cases where rapid TEC variations are expected as in sector (i), estimations of missing values were done when at least half of the total expected number of data points were filled with TEC data. For example, when there were at least 4 measurements in sector (ii) the missing values were obtained by evaluating a spline function fitted through the existing TEC data values. On the other hand, when there were at least 7 (half the number of hours during 10:00 – 24 LT) TEC values in sector (i), the missing values were obtained by evaluating a spline function fitted to the available data values. After estimating the missing TEC data from the two sections of the diurnal TEC, the entire diurnal TEC data over a particular grid cell was then considered to estimate the missing values. When there were at least 12 (half the number of hours in a day) values, the missing values were obtained by evaluating a spline function fitted to the existing data values.

2. At a particular latitude and local time, the values of TEC along all the longitudes were divided into western (-20 – 20^{o} E) and eastern (20 – 60^{o} E) longitude sectors. Each of the longitude sectors contained 8 bins. At night, when there were at least 3 TEC values over any longitude sector, the missing values were obtained by evaluating spline function fitted to the available data points, while during the day, when there were at least 4 Tec values, the missing values were obtained by evaluating a spline function fitted to the available data points. After

estimating the missing TEC values over the two longitude sectors, the TEC over all longitudes were then considered to estimate the missing values. At night, when there were at least 8 values, the remaining values where obtained by evaluating a spline fitted to the available TEC data points. The missing values during day time, were estimated when there were at least 10 measurements available.

3. Procedure 3 is similar to 2, except for variations of TEC as a function of latitude were considered at specific values of longitude and time. TEC values over the latitudes were divided into lower (-35 – 0° S) and upper (0 – 35° N) latitudinal sectors. There were 12 bins in each of the latitudinal sector. To estimate missing TEC values at night over a latitudinal sector, at least 4 measurements were required to be available, while during the day, at least 6 values were required. When TEC data over the combined latitudinal sectors were considered to estimate the missing values, at least 12 values were required to be available.

After repeating procedures 1 – 3 three times, all the 3,981,312 bins were filled with TEC data and they were used to obtain the model coefficients as explained in section 3.

3. The Model

The TEC over the African region was expressed as

$$TEC(t,d,F,\lambda,\phi) = \sum_{i=1}^{24}\sum_{j=1}^{12}\sum_{k=1}^{36}\sum_{l=1}^{16}\sum_{m=1}^{24} a_{ijklm} \times N_i(t) \times N_j(d) \times N_k(F) \times N_l(\lambda) \times N_m(\phi) \quad (1)$$

where the linear model coefficients a_{ijklm} were determined by the least square fitting procedure to the 3,981,312 TEC data values as in Abdu et al. (2003); Jakowski et al. (2011b); Mungufeni et al. (2015). In Equation 1, $N_i(t)$, $N_j(d)$, $N_k(F)$, $N_l(\lambda)$, and $N_m(\phi)$ are B splines of different orders to represent variations of TEC with local time, seasons, solar flux level, longitude, and latitude respectively. Most of the B splines were of order 2, except for those used to represent LT and latitudinal variations which were of order 4. The order of splines used to represent LT and latitude was higher to cater for

the rapid variations of TEC with these two parameters. Twenty-four local time nodes 1, 2, ..., 24 were used. For simple interpolation between months, seasonal/monthly nodes were placed at the 15th day of each month. Solar flux nodes used in the various months are as shown in Table 2. The longitudinal nodes were separated by 5^o and placed at longitudes -17.5, 12.5 7.5, ..., 57.5 degrees, while the latitudinal nodes were separated by 3^o and placed at latitudes -34.5, -31.5, -28.5, … , 34.5 degrees.

4. Comparison of Observed and Modeled TEC

In order to assess the ability of the model to describe the data used to construct it, modelled data were compared with the binned data that were used to solve equation 1. The results of the self-consistency check are presented in Figure 1. It is important to note that validation using data that was not included during modeling is provided in section 5. Panels in column (i) of Figure 1 present the observed binned TEC data while column (ii) presents the corresponding modeled TEC data. In column (iii), we present the differences between the observed and modeled TEC data, referred to as errors. In Figure 1, rows (a), (b), and (c) correspond to LSA, MSA, and HSA, respectively. The horizontal magenta lines in Figure 1 and later also in Figure 2 indicate the location of ~0^o dip latitude on the corresponding panel. As expected, Figure 1 clearly shows that the corresponding modeled TEC almost perfectly matches the observed binned TEC. This can be confirmed by the small (<0.1 TECU) error values presented in panels of column (iii). The variations of the ionosphere with local time, solar flux level as well as location that are exhibited in Figure 1 gives the confidence of relying on the binned data as a good representation of the ionosphere. The physical explanations for these variations are as follows. The increase of both observed and modeled TEC that occurs when solar flux level increases is usually attributed to increased ionizing radiations in X-ray and Extreme Ultra-Violet (EUV) bands, which in turn leads to increased TEC in the ionosphere (Hargreaves, 1992).

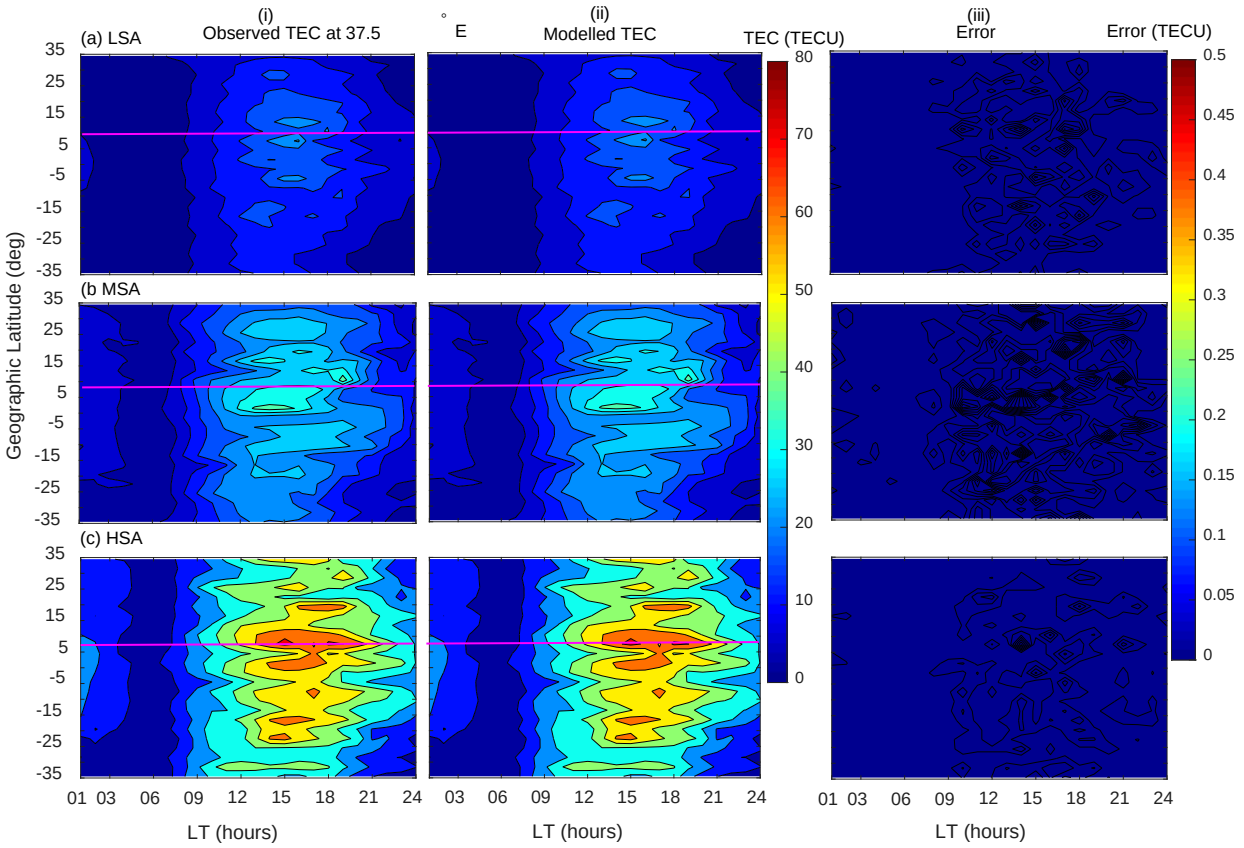

Figure 1**.** Variation of TEC as a function of geographic latitude and local time in March equinox at 37.5^{o} E. Panels in rows (a) - (c) correspond to LSA, MSA, and HSA, respectively, while panels in columns (i) - (iii) correspond to observed binned, modeled TEC, and difference between observed and modeled TEC (errors), respectively. Magenta line indicates ~0^{o} dip latitude.

The diurnal variation of TEC matches very well with the variation of photo-ionising radiations. At sunrise, the electron density begins to increase rapidly owing to photo-ionization (Schunk and Nagy, 2009). After this initial increase at sunrise, electron density displays a slow rise throughout the day, and then it decays at sunset as the photo-ionization source disappears. Another diurnal feature of variation of TEC exhibited in Figure 1 is the existence of a secondary maximum of TEC. This can clearly be seen in panels of row (c) along the magenta lines, where the first peak occurs at ~15:00 LT and the second at ~18:00 LT. The formation of a secondary maximum of TEC that was mentioned previously may be explained as follows. During the day, the thermospheric wind generates a dynamo electric field in the lower ionosphere that is eastward (Schunk and Nagy, 2009). The eastward electric field, E in combination with

the northward geomagnetic field, B produces an upward E×B drift of the F region plasma. As the ionosphere co-rotates with the Earth toward dusk, the zonal (eastward) component of the neutral wind increases. The increased eastward wind component, in combination with the sharp day-night conductivity gradient across the terminator leads to the pre-reversal enhancement in the eastward electric field (Batista et al., 1986; Schunk and Nagy, 2009). The F layer therefore rises as the ionosphere co-rotates into darkness. Although in the absence of sunlight after sunset, the lower ionosphere rapidly decays, there exists high electron density at high altitudes, yielding the secondary maximum in TEC.

Panels in rows (b) and (c) of Figure 1 demonstrate the existence of the EIA region, where there exist two belts of high electron density on both sides of 0^{o} dip latitude. The EIA is usually attributed to the upward *E*×*B* drift which lifts plasma to higher altitudes. The plasma then diffuses north and south along magnetic field lines. Due to gravity and pressure gradient forces, there is also a downward diffusion of plasma. The net effect is the formation of the EIA region (Appleton, 1946). Another feature of EIA that can be seen on panels in rows (b) and (c) of Figure 1 is the asymmetry of the crests. Along 120^{o} longitude sector Zhang et al. (2009) reported the asymmetry of EIA crests. As described later at the end of this section, the direction of neutral meridional winds in March may favour high values of electron density over the southern crest.

Generally, Figure 1 shows that, the locations outside the EIA region have lower TEC values compared to locations around and within the EIA region. The low values of TEC over locations outside the EIA region might be due to lower elevation angle of solar radiation flux which is responsible for creation of electrons (Schunk and Nagy, 2009). The solar radiation flux is usually low for locations far from the sub-solar point. The latter situation is dominant over locations outside the EIA region, especially in March. The closeness of the sub-solar point to the locations within the EIA regions result into high solar radiations over these locations. As a result, high TEC values were observed over locations within the EIA region.

To demonstrate that the modeled TEC captures TEC variation with seasons, we present Figure 2. In the figure, columns (i) and (ii) present observed binned and the corresponding modeled TEC respectively. Moreover, rows (a) - (d) present TEC data during March, June, September and December, respectively.

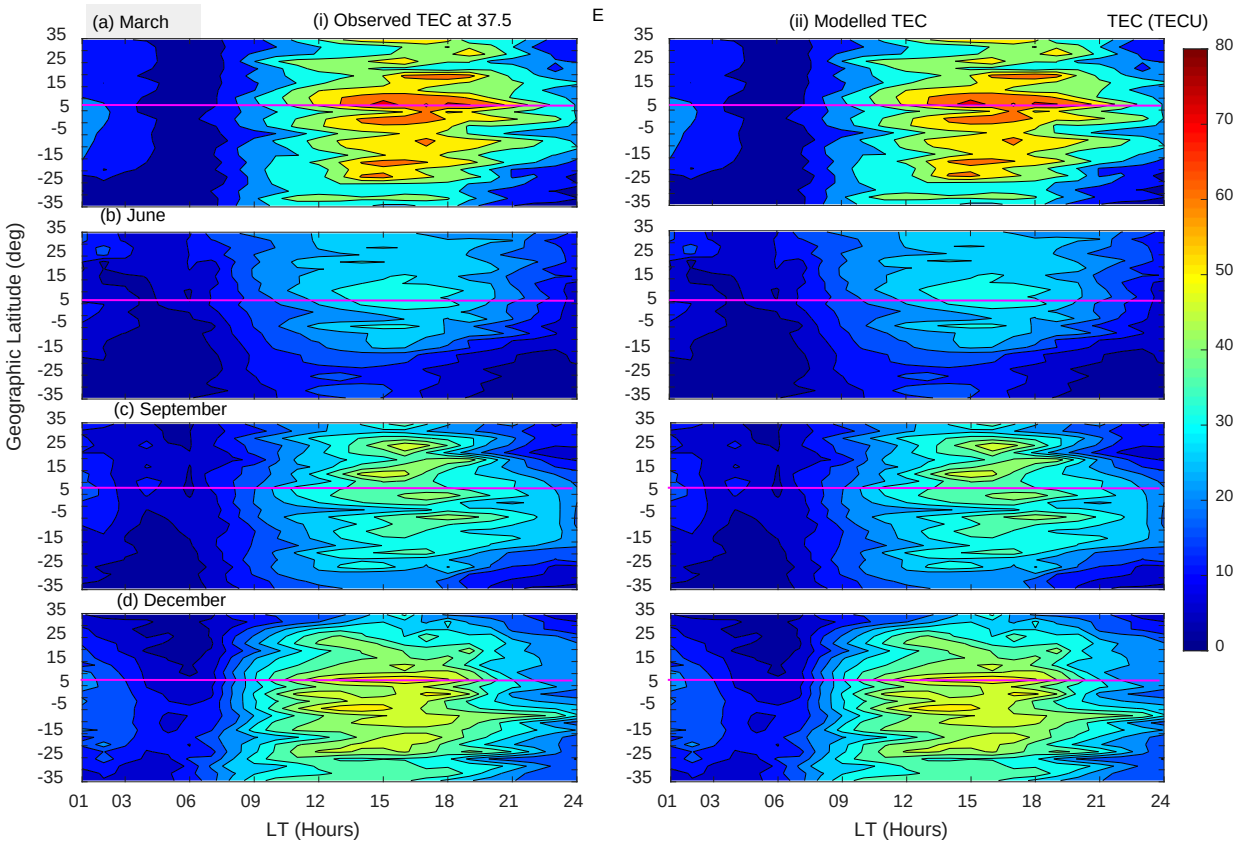

Figure 2**.** Variation of TEC as a function of latitude and local time in HSA at 37.5^{o}E. Panels in rows (a) - (d) are for March equinox, June solstice, September equinox, and December solstice respectively, while panels in columns (i) and (ii) are observed binned and modeled TEC respectively. Magenta line indicates 0^{o} dip latitude.

As already observed in Figure 1, it can clearly be seen from Figure2 that the modeled TEC almost perfectly matches the observed TEC data. Among the many features of TEC exhibited by both observed and modeled TEC data, we would like to emphasize the (i) equinoxial asymmetry of TEC, (ii) occurrence of lowest TEC in June solstice, and

(iii) high values of TEC in December. Features (ii) and (iii) were recently reported based on a similar data by Mungufeni et al. (2019). The reader may refer to this study for more discussions. Mungufeni et al. (2016a) observed equinoxial asymmetry when studying ionospheric irregularities over the African low latitude region. They observed over the East African region that, the irregularity strength in March equinox was higher than that in September equinox. They attributed the equinoxial asymmetry to meridional winds in March which might blow northward. Such a direction would lift plasma up where recombination is not common. On the other hand, in September, the winds might blow southward. This could lead to recombination at low altitudes.

5. Model Validation

5.1 Validation using reserved COSMIC RO TEC

In addition to comparing observed binned TEC with the corresponding modeled TEC, we validated our model using observed TEC in the years 2012 and 2018. The data during these two years were not used in developing the model. The TEC data in the years 2012 and 2018 were binned according to local time and spatially in a similar manner to that mentioned in subsection 2.2. The corresponding local time, day of the year, solar flux, and spatial coordinates of the data were noted and then used to generate the corresponding modeled TEC. Figure 3 presents a scatter plot showing the observed TEC against the corresponding modeled TEC. The red line in the figure indicates linear least squares fit to the data in the panel. Furthermore, indicated in Figure 3 are: (i) the correlation coefficients, r, (ii) the r squared values, (iii) the number of data points, n plotted and (iv) the root mean squared error, RMSE when the modeled TEC is used to represent the observed TEC.

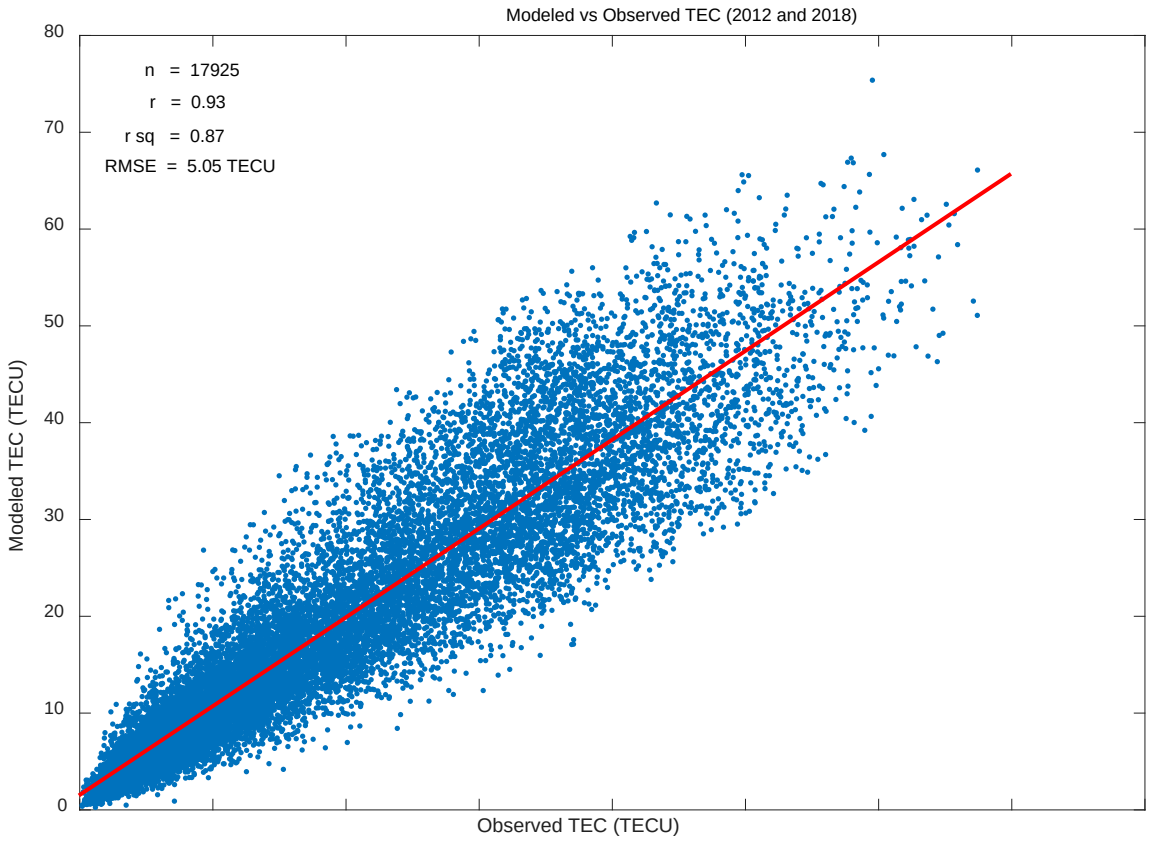

Figure 3**.** Scatter plot of observed TEC against modeled TEC.

The following observations can be noted from Figure 3. (i) The modeled TEC correlates highly (r ~0.93) with the observed TEC. (ii) The r squared values indicate that high proportions (~87 %) of the variations in the observed TEC can be predicted by the modeled TEC. (iii) The RMSE value of 5.05 TECU signify that the modeled TEC closely approximates the observed TEC.

In order to show that the observed and modeled TEC have similar magnitudes in addition to their similar variation depicted in Figure 3, we computed the differences between corresponding values of the data plotted in the figure. These were referred to as errors. We also computed the percentage of the different errors. The left and right hand vertical axis in Figure 4 present the distribution of the number of observed errors and their percentages, respectively. It can be seen from the figure, the errors are

randomly distributed since the distribution curve is symmetric about 0 TECU. Indeed, the magnitudes of the modeled TEC values are close to that of the observed TEC since the majority of the error values are close to zero.

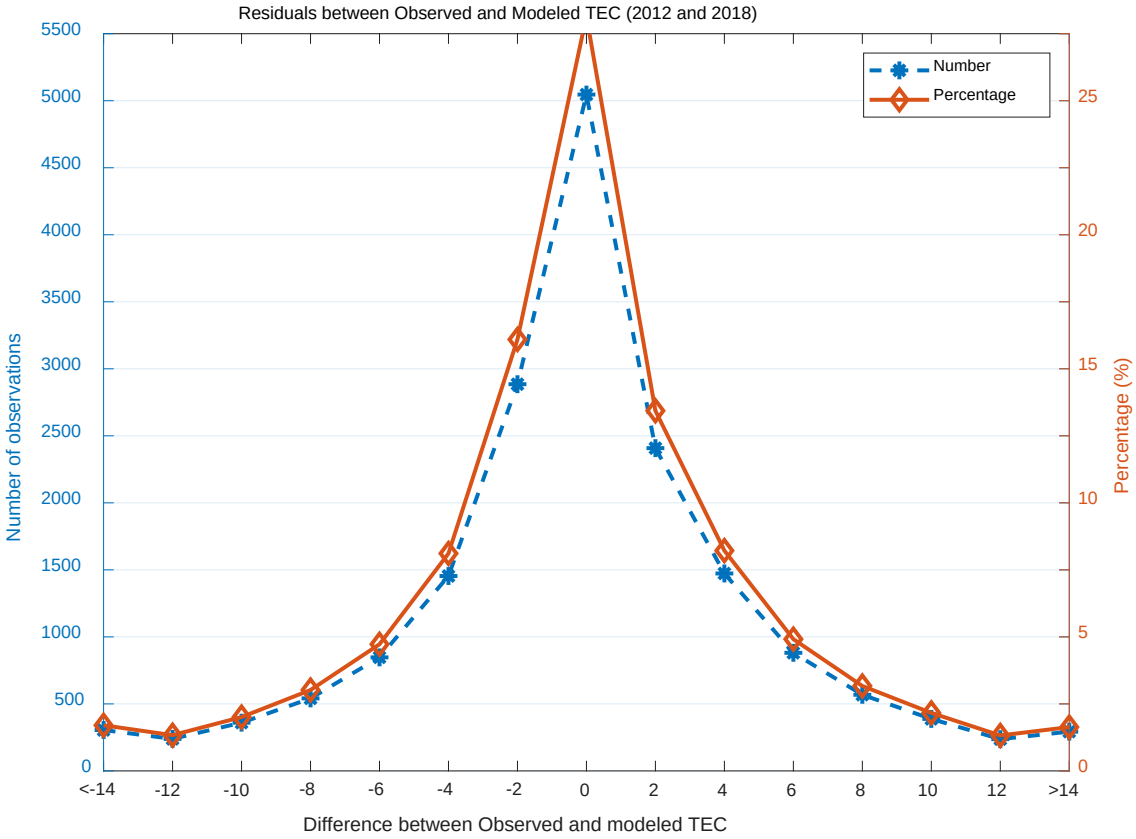

Figure 4**.** The blue and red curves show the distribution of the number of observed errors (difference between observed and modeled TEC) and the percentage of the errors, respectively. The cases of high error values (> 10 TECU) as seen on the right-hand side vertical axis mostly have < 2.5 % occurrence probability.

5.2 Validation using ionosonde TEC measurements

The TEC data measured by the digisonde ionosonde stations over South Africa located at Hermanus, Grahamstown and Louisvale can be accessed from the National Oceanic and Atmospheric Administration (NOAA) website via the link, ftp://ftp.ngdc.noaa.gov. The data obtained from the NOAA website is in form of auto-scaled ionospheric parameters such as peak height in F2 layer, critical frequency in F2 layer, and TEC which are stored in Standard Archiving Output (SAO) format files. It should be noted that the TEC data provided in SAO files are obtained by integrating electron density profiles up to altitude of ~700 km. More details about the auto-scaling program (real-time ionogram scaler with true height (ARTIST)) and the electron density profiles they produce can be found in Reinisch and Huang (2001) and Klipp et al. (2020).

Figure 5 presents with magenta lines the diurnal patterns of TEC measured by ionosonde stations at Hermanus (panels in column (i)), Grahamstown (panels in column (ii)) and Louisvale (panels in column (iii)). The corresponding TEC generated by our spline technique model (spline), Nequick 2, and IRI-2016 are superimposed with red, green and blue lines, respectively. We need to mention that during computation of TEC using NeQuick 2 and IRI-2016, the height was limited to the approximate altitude of the COSMIC satellites (800 km). The panels in rows (a) - (c) show TEC on day of year 170 (June), 260 (September), and 350 (December), respectively. All these three days of the year 2013 were geomagnetically quiet. Preliminarily, Figure 5 appears to reveal that IRI-2016 either overestimates (December) or underestimates (June and September) the TEC measured by the ionosonde stations. On the other hand, our spline model and NeQuick 2 seem to depict good correspondence between the observed and the modeled TEC. It can also be seen from Figure 5 that over a particular station, the shape of curves on different days representing TEC generated by the IRI-2016 and NeQuick 2 models are similar. This is expected since these two models were meant to reproduce monthly median values of the ionosphere. This means that our model, based on spline functions may capture better the day-to-day variability of the ionosphere.

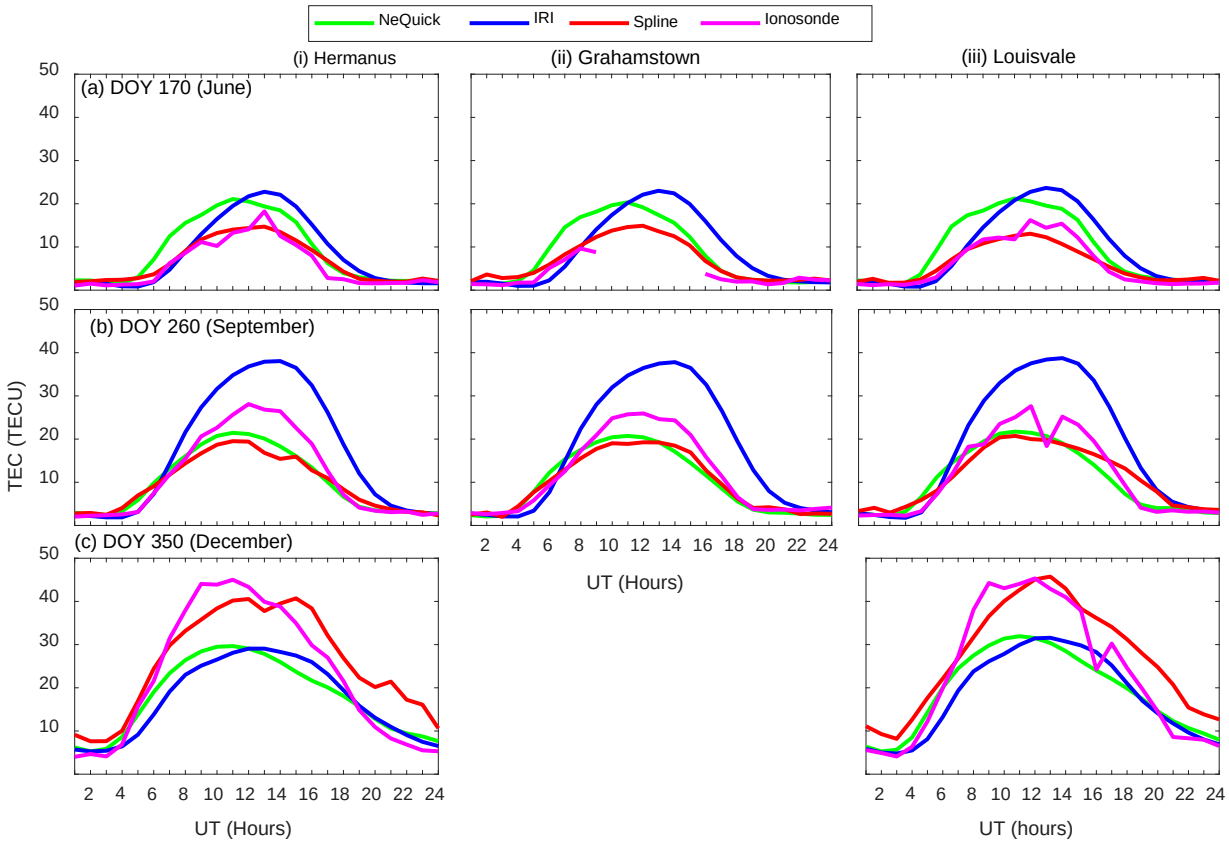

Figure 5: Magenta color shows diurnal TEC observed by ionosonde stations at Harmanus (panels in column (i)), Grahamstown (Panels in column (ii)), and Louisvale (Panels in column (iii)). The green, blue, and red colors show TEC estimations using NeQuick 2, IRI-2016 and Spline models, respectively. Panels in rows (a) - (c) show diurnal TEC during the year 2013 on DOY 170, 260, and 350, respectively.

We generated such data plotted in Figure 5 for geomagnetically quiet days of the entire year 2013 and then performed statistical analysis of the observed and the model TEC data. Table 3 presents in columns 3 the correlation coefficients, r for the correlations between modeled and ionosonde TEC. Moreover, the table presents the RMSE when the ionosonde TEC was estimated using the models listed in column 2. The number of observations, n over each station that were used to determine, r and RMSE are put in brackets below the station name.

Table 3: Correlation coefficients, r and RMSE associated with estimation of TEC observed by ionosonde stations using models

Ionosonde Station /number of observations	Model	r	RMSE (TECU)
Hermanus (n = 5,110)	Spline	0.92	4.64
	IRI-2016	0.86	5.45
	NeQuick 2	0.92	4.10
Grahamstown (n = 4,450)	Spline	0.88	5.56
	IRI-2016	0.82	6.29
	NeQuick 2	0.86	5.27
Louisville (n = 4,543)	Spline	0.94	3.82
	IRI-2016	0.87	5.62
	NeQuick 2	0.94	3.73

It can be seen from Table 3 that the r values associated with NeQuick 2 and spline based model are consistently better when compared with that of IRI-2016. Moreover, the RMSE values associated with IRI-2016 are the highest in all the cases. These two observations indicate that compared to spline and NeQuick 2, IRI-2016 poorly estimates TEC at the locations of the ionosondes. The RMSE values associated with NeQuick 2 are always slightly lower than that of spline, while the r values associated with spline are mostly comparable or slightly higher than that of NeQuick 2. These discussions demonstrate that our spline model generates TEC values consistently with that observed by ionosondes. This implies that equivalent TEC measured by ionosondes over locations which do not have ionosonde stations can be predicted fairly well using our model.

5.3 Comparison of our model with existing regional models

It would be good to compare error levels produced when some measured TEC are compared with modeled TEC generated by (i) the existing regional TEC models discussed in section 1 and (ii) our spline technique TEC model. We may not perform such analysis since models in (i) are based on electron density integrated from ground up to GPS satellites (~20,200 km), while model in (ii) is based on electron density integrated up to ~800 km. However, we present Figures 6 and 7 to compare EIA features captured by our spline technique model and the neural networks technique of Okoh et al. (2019). The TEC plots based on the neural networks technique can be obtained from MATLAB Central website (Okoh et al., 2019) (https://www.mathworks.com/matlabcentral/fileexchange/69257-african-gnss-tec-afritec-model?s_tid=prof_contriblnk). We present in Figure 6 examples of TEC generated by neural network model during the year 2012 at 11:00 UT. Over the East African sector (LT = UT + 3), this time translates to 14:00 LT and falls within the range of LT when EIA exists over the region (Mungufeni et al., 2018). Panels (a) and (b) in Figure 6 present TEC during March (DOY 81) and September (DOY 260) equinoxes, respectively, while (c) and (d) present during June (DOY 171) and December (DOY 347) solstices, respectively. It is important to mention that these 4 days were geomagnetically quiet.

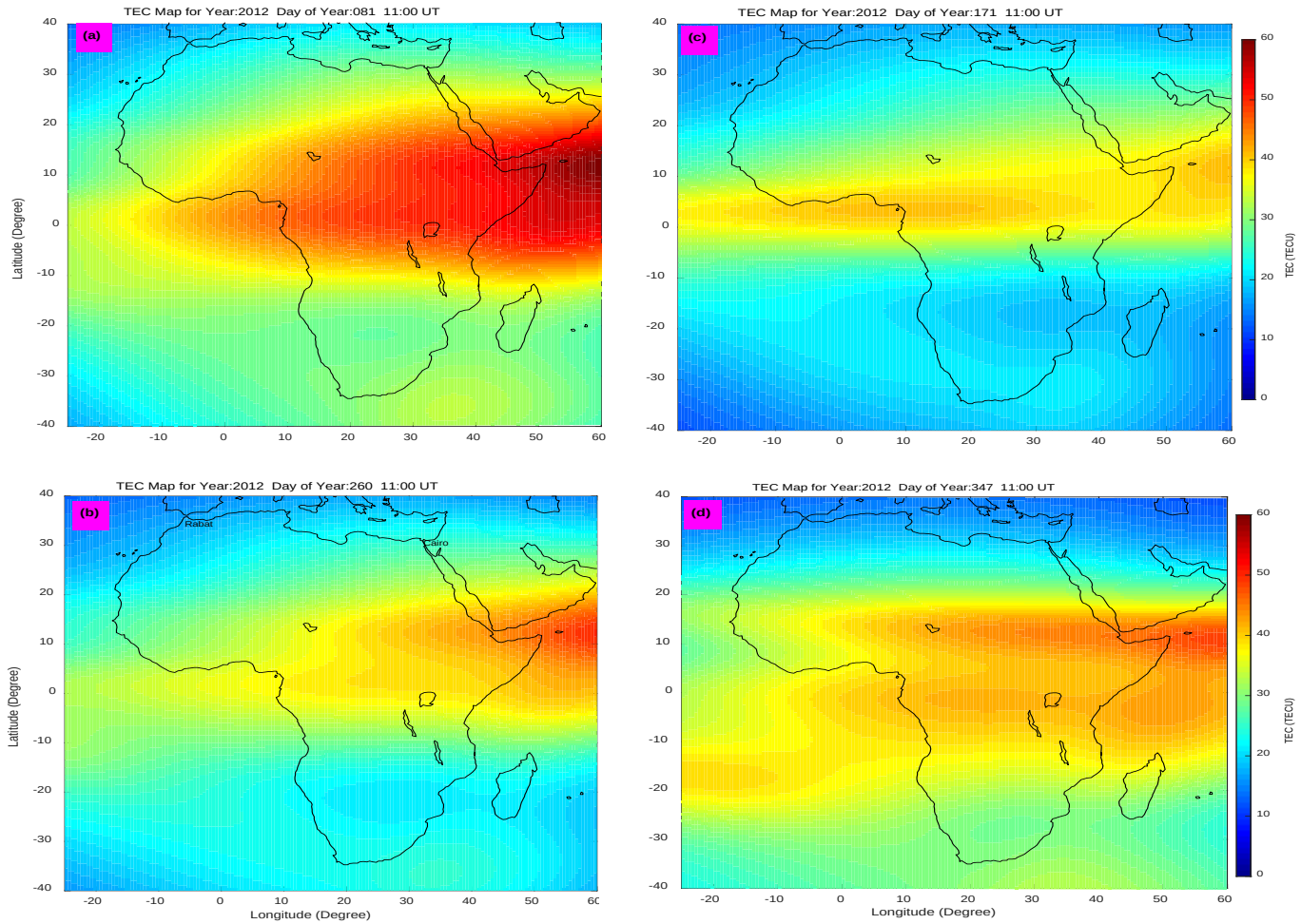

Figure 6: Neural Network TEC maps during the year 2012 at 11:00 UT. Panels (a) and (b) are for March (DOY 81) and September (DOY 260) equinoxes, respectively, while (c) and (d) are for June (DOY 171) and December (DOY 347) solstices, respectively.

In order to generate TEC maps using our model for purposes of comparing with TEC maps in Figure 6, we noted and used the F10.7 flux values on the days indicated in the figure. The TEC maps generated using our model that correspond to TEC maps presented in Figure 6 are presented in Figure 7.

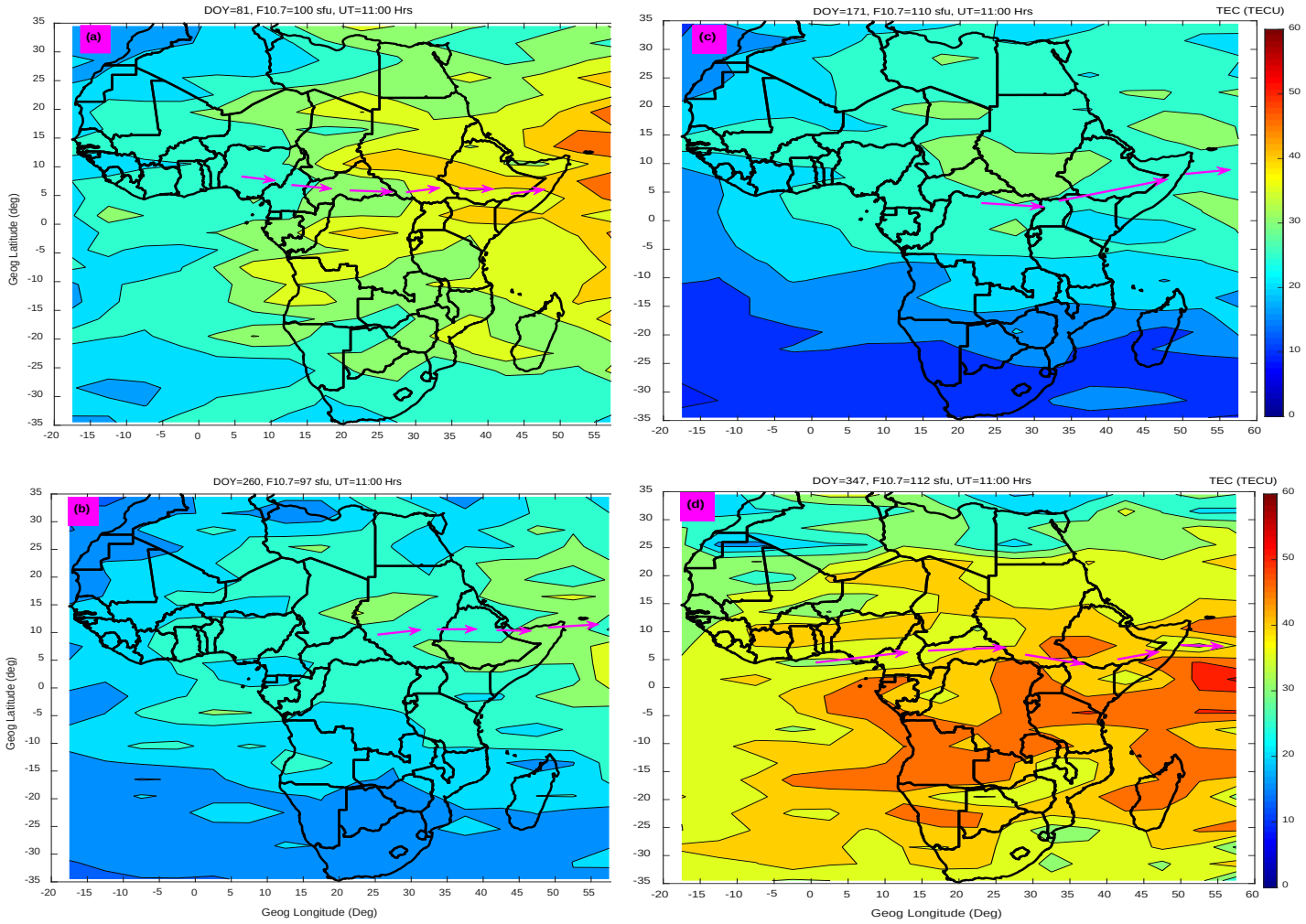

Figure 7: Similar to Figure 6, but generated by spline modeling technique. Magenta arrows indicate approximate locations of EIA trough.

Unlike our TEC maps in Figure 7 which clearly show the EIA trough (see magenta arrows) in all the seasons, the neural network technique TEC maps (Okoh et al., 2019) of Figure 6 only clearly capture the EIA trough in December solstice. As pointed before, this short fall in neural network TEC model might be due to poor amount of data to represent day of year during model development. Another observation that can be made from Figures 6 and 7 is that unlike the neural network model which yields smooth spatial TEC variation, the spline modeling technique does not yield smooth spatial TEC variation. In real life, measurement or observed values rarely vary smoothly. Since the

spline modeling technique produces results (see Figure 1) which demonstrate that the modeled data matches almost perfectly the observed data, it is expected that the spatial variations of TEC in maps of Figure 7 are not smooth.

6. Conclusions

This study developed a model of TEC measured by COSMIC satellites. The TEC data were binned according to local time, seasons, solar flux level and spatially. The coefficients of B splines that were fitted to the binned data were determined by means of the least square procedure. As expected, the modeled TEC almost perfectly matched the corresponding observed binned TEC data. The model was validated with independent data that were not used in the model development. The validation revealed that (i) the observed and the modeled TEC correlate highly (r = 0.93), (ii) the coefficient of determination R^2 which is the proportion of variance in the observed data predicted by our model was 87 %, and (iii) the modeled TEC closely approximates the observed TEC (RMSE of 5.02 TECU). Due to the extensive input data and the applied modeling technique, we were able to reproduce the well-known features of TEC variation over the African region. Further validation of our model using TEC obtained from ionosonde stations over South Africa at Hermanus, Grahamstown and Louisville reported r values > 0.92 and RMSE < 5.56 TECU. These validation results imply that our model can estimate fairly well TEC that would be measured by ionosondes over locations which do not have the instrument.

Acknowledgments

This study received financial support from research number, 018-1370-20 in the department of Astronomy and Space Science of Chungnam National University which was awarded by the Air Force Research Laboratory of the United States of America. The first author, Patrick Mungufeni greatly appreciates the immense contribution of Prof.

Claudia Stolle towards shaping the presentation of the manuscript. We thank the developers of the IRI and NeQuick models for making their models available. Dst data is provided by the World Data Center for Geomagnetism at Kyoto (http://swdcwww.kugi.kyoto-u.ac.jp/). Kp data isprovided by GFZ Potsdam, ftp://ftp.gfz-potsdam.de/pub/home/obs/kp-ap/. F10.7 flux data was obtained from http://www.swpc.noaa.gov/, while ionPrf files used to derive COSMIC TEC were obtained from http://cosmic-io.cosmic.ucar.edu/cdaac/index.html. We thank NOAA for availing ionosonde data via the link, ftp://ftp.ngdc.noaa.gov.

References

Abdu, M. A., Souza, J. R., Batista, I. S., and Sobral, J. H. A.: Equatorial spread F statistics and empirical representation for IRI: A regionalmodel for the Brazilian longitude sector, Adv. Space Res., 31, pp. 703 – 716, 2003.

Adewale, A. O., Oyeyemi, E. O., Adeloye, A. B., Ngwira, C. M., and Athieno, R.: Responses of equatorial F region to different geomagneticstorms observed by GPS in the African sector, J. Geophys. Res., 116, A12319, doi:10.1029/2011JA016998, 2011.

Appleton, E. V.: Two Anomalies in the Ionosphere, Nature, p. 691, 1946.

Batista, I. S., Abdu, M. A., and Bittencourt, J. A.: Equatorial F region vertical plasma drifts: seasonal and longitudinal asymmetries in the American sector, J. Geophys. Res., 91, pp. 12055 – 12064, 1986.

Bilitza, D.: International Reference Ionosphere 2000, Radio Sci., 36, pp. 757 – 767, 2001.

Bolaji, O., Owolabi, O., Falayi, E., Jimoh, E., Kotoye, A., Odeyemi, O., Rabiu, B., Doherty, P., Yizengaw, E., Yamazaki, Y., Adeniyi, J., t Kaka, R., and Onanuga, K.: Observations of equatorial ionization anomaly over Africa and Middle East during a year of deep minimum, Ann. Geophys., 35, pp. 123 – 132, 2017.

Buonsanto, M. J.: Ionospheric Storms – A Review, Space Sci. Rev., 88, pp. 563–601, 1999.

De-Boor, C. *A Practical Guide to Splines*. Springer-Verlag, New York, 1978.

Emmert, J. T., Richmond, A. D., and Drob, D. P.: A computationally compact representation of Magnetic-Apex and Quasi-Dipole coordinates with smooth base vectors, J. Geophys. Res., 15; A08322; doi:10.1029/2010JA015326, 2010.

Ercha, A., Zhang, D., Ridley, A. J., Xiao, Z., and Hao, Y.: A global model: Empirical orthogonal function analysis of total electron content 1999–2009 data, J. Geophys. Res., 117, doi:10.1029/2011JA017238, 2012.

Guochang, X.: GPS. Theory, Algorithms, and Applications, Springer-Verlag, pp. 43, 2007.

Habarulema, J.B., M. L. O. B.: Regional GPS TEC modeling; attempted spatial and temporal extrapolation of TEC using neural networks, J. Geophys Res: Space Phys., 116, A04314, 2011.

Hargreaves, J. K.: The Solar-Terrestrial environment, Cambridge University Press., New York, pp. 208, 1992.

Hofmann-Wellenhof, B., Lichtenegger, H., and Wasle, E.: Global Navigation Satellite Systems, GPS, GLONASS, Galileo and more, Springer Wien New York, pp. 105, 2007.

Jakowski, N., Hoque, M. M., and Mayer, C.: A new global TEC model for estimating trans-ionospheric radio wave propagation errors, J. Geod., 85, pp. 965 - 974, 2011a.

Jakowski, N., Schlüter, S., and Sardon, E.: Total electron content models and their use in ionosphere monitoring, Radio Sci., 46, RS0D18, doi:10.1029/2010RS004620, 2011b.

Klipp, T. d. S, Petry, A, de Souza, J. R, de Paula, E. R, Falcão, G. S, and Velho, H. F. d-C: Ionosonde total electron content evaluation using International Global Navigation Satellite System Service data, Ann. Geophys., 38, pp: 347 – 357, 2020.

Klobuchar, J. A: Ionospheric time-delay algorithm for single frequency GPS users. IEEE Trans Aerosp Electron Syst. 23,(3), pp. 325 - 331. Doi.org/10.1109/TAES.1987.3-10829, 1987.

Krankowski, A., Zakharenkova, I., Krypiak-Gregorczyk, A., Shagimuratov, I. I., Wielgosz, P: Ionospheric electron density observed by FORMOSAT-3/COSMIC over the European region and validated by ionosonde data. *Journal of Geodesy*, *85*(12), pp. 949 - 964. https://doi.org/10.1007/s00190-011-0481-z, 2011

Leva, J. L., de Haag, M. U., Dyke, K. V.: Performance of standalone GPS. In Kaplan, E. D. and Hegarty, C. J., editors, *Understanding GPS: Principles and Applications*, p. 66 – 112, Artech House INC., 2006.

Mengist, C. K., Ssessanga, N., Jeong, S.-H., Kim, J.-H., Kim, Y. H., & Kwak, Y.-S: Assimilation of multiple data types to a regional ionosphere model with a 3D-Var algorithm (IDA4D). *Space Weather*, *17*, pp. 1018 - 1039. https:// doi.org/10.1029/2019SW002159, 2019.

Mukhtarov, P., Pancheva, D., Andonov, B., and Pashova, L.: Global TEC maps based on GNSS data: 1. Empirical background TEC model, J. Geophys. Res: Space Phys., 118, pp. 4594 - 4608, 2013.

Mungufeni, P., Jurua, E., Habarulema, J. B., and Anguma, S. K.: Modeling the probability of ionospheric irregularity occurrence over African low latitude region, J. Atmos. Sol.-Terr. Phys., 128, pp. 46 - 57, 2015.

Mungufeni, P., Habarulema, J. B., and Jurua, E. a.: Trends of ionospheric irregularities over African low latitude region during quiet geomagnetic conditions, J. Atmos. Sol.-Terr. Phys., 14, pp. 261–267, 2016a.

Mungufeni, P., Habarulema, J. B., Migoya-Orué, Y., and Jurua, E.: Statistical analysis of the correlation between the equatorial electrojet and the occurrence of the equatorial ionisation anomaly over the East African sector, Ann. Geophys., 36, pp. 841 – 853, 2018.

Mungufeni, P., Rabiu, A. B., Okoh, D., and Jurua, E.: Characterization of Total Electron Content over African region using Radio Occultation observations of COSMIC satellites, Adv. Space Res., doi:10.1016/j.asr.2019.08.009, 2019.

Najman, P. and Kos, T.: Performance Analysis of Empirical Ionosphere Models by Comparison with CODE Vertical TEC Maps, Chapter 13, in: Mitigation of Ionospheric Threats to GNSS: an Appraisal of the Scientific and Technological Outputs of the TRANSMIT Project, InTech Open Science publications, pp. 162 - 178, doi:10.5772/58774, 2014.

Nava, B., Coïsson, P., and Radicella, S. M.: A new version of the NeQuick ionosphere electron density model, J. Atmos. Sol. Terr. Phys., 70 (15), pp.1856 – 1862, 2008.

Okoh, D., Owolabi, O., Ekechukwu, C., Folarin, O., Arhiwo, G., Agbo, J., Bolaji, S., and Babatunde, R.: A regional GNSS-VTEC model over Nigeria using neural networks: A novel approach, Geodesy and Geodynamics, 7 (1), pp. 19 - 31, 2016.

Okoh, D, Seemala, G, Rabiu, B, Habarulema, J. B., Jin, S., Shiokawa, K., Otsuka, Y., et al., (2019). A Neural Network-Based Ionospheric Model Over Africa From Constellation Observing System for Meteorology, Ionosphere, and Climate and Ground Global Positioning System Observations, JGR: Space Physics, 124, https:// doi.org/10.1029/2019JA027065.

Opperman, B.: Reconstructing ionospheric TEC over South Africa using signals from a regional GPS network, Rhodes Univ., Ph. D. Thesis, pp. 30, Grahamstown, South Africa., 2008.

Rama Rao, P. V. S., Jayachandran, P. T., Sri Ram, P., Ramana Rao, B. V., Prasad, D. S. V. V. D., and Bose, K. K.: Characteristics of VHF radiowave scintillations over a solar cycle (1983 - 1993) at a low-latitude station: Waltair (17.7^{o}N, 83.3^{o}E), Ann. Geophys, 15, pp. 729 – 733, 1997.

Reinisch, B. and Huang, X.: Deducing topside profiles and total electron content from bottomside ionograms, Adv. Space Res., 27, pp: 23 – 30, doi:10.1016/S0273-1177(00)001368, 2001.

Rishbeth, H. and Garriot, O. K.: Introduction to Ionospheric Physics, pp 47, Academic Press, New York, 1969.

Schunk, W. R. and Nagy, F. A.: Ionospheres: Physics, Plasma Physics, and Chemistry, pp. 335 396, Cambridge University press, New York, 2nd ed., 2009.

Sun, Y., Liu, J., Tsai, H., and Krankwski, A.: Global ionospheric map constructed by using TEC from ground-based GNSS receiver and FORMSAT-3/COSMIC GPS occultation experiment, GPS solutions, doi:10.1007/s10291-017-0635-4, 2017.

Tebabal, A., Radicella, S. M., Damtie, B., Migoya-Orue', Y., Nigussie, M., and Nava, B.: Feed forward neural network based ionosphericmodel for the East African region, J. Atmos. Sol. Terr. Phys., 191, pp. 1 – 10, doi:10.1016/j.jastp.2019.05.016, 2019.

Thébault, E., Finlay, C. C., Beggan, C. D., Alken, P., Aubert, J., Barrois, O., Bertrand, F., Bondar, T., and Bones, A.: International Geomagnetic Reference Field: the 12th generation, Earth, Planets and Space, pp. 67-79, doi:10.1186/s40623-015-0228-9, 2015.

Zhang, M.-L., Wan, W., Liu, L., and Ning, B.: Variability study of the crest-to-trough TEC ratio of the equatorial ionization anomaly around120^{o}E longitude, Adv. Space Res., 43, pp. 1762 – 1769, 2009.